M. Tech (Power Electronics and Systems)

Archit Chauhan

2024

ACTIVE CELL BALANCING WITH ZCS SWITCHED-CAPACITOR AND MODULARIZED BUCK-BOOST + CUK CONVERTER FOR LITHIUM-ION BATTERIES

DISSERTATION/THESIS

SUBMITTED IN PARTIAL FULFILLMENT OF THE
REQUIREMENTSFOR THE AWARD OF THE DEGREE
OF

MASTER OF TECHNOLOGY
IN
POWER ELECTRONICS & SYSTEMS

Submitted by:

ARCHIT CHAUHAN

2K22/PES/05

Under the supervision of

DR. SUDARSHAN KUMAR BABU VALLURU
(Professor, EED, DTU)

DR. VANJARI VENKATA RAMANA
(Assistant Professor, EED, DTU)

DEPARTMENT OF ELECTRICAL ENGINEERING
DELHI TECHNOLOGICAL UNIVERSITY
(Formerly Delhi College of Engineering)
Bawana Road, Delhi-110042

MAY, 2024

DEPARTMENT OF ELECTRICAL ENGINEERING
DELHI TECHNOLOGICAL UNIVERSITY
(Formerly Delhi College of Engineering)
Bawana Road, Delhi-110042

CANDIDATE'S DECLARATION

I, **ARCHIT CHAUHAN**, Roll No. 2K22/PES/05 student of M. Tech (Power Electronics &Systems), hereby declare that the project Dissertation titled **"Active Cell Balancing With ZCS Switched-Capacitor And Modularized Buck-Boost + Cuk Converter For Lithium-Ion Batteries"** which is submitted by me to the Department of Electrical Engineering Department, Delhi Technological University, Delhi in partial fulfillment of therequirement for the award of the degree of Master of Technology, is original and not copiedfrom any source without proper citation. This work has not previously submitted for the award of any Degree, Diploma Associateship, Fellowship, or other similar title or recognition.

Place: Delhi **(Archit Chauhan)**
Date: 31/05/2024

DEPARTMENT OF ELECTRICAL ENGINEERING
DELHI TECHNOLOGICAL UNIVERSITY
(Formerly Delhi College of Engineering)
Bawana Road, Delhi-110042

CERTIFICATE

I hereby certify that the project Dissertation titled **"Active Cell Balancing With ZCS Switched-Capacitor And Modularized Buck-Boost + Cuk Converter For Lithium-Ion Batteries"** which is submitted by Archit Chauhan, Roll No. 2K22/PES/05, Department of Electrical Engineering, Delhi Technological University, Delhi in partial fulfilment of the requirement for the award of the degree of Master of Technology, is a record of the project work carried out by the student under my supervision. To the best of my knowledge this work has not been submitted in part or full for any Degree or Diploma to this University or elsewhere.

Place: Delhi
Date: 31/05/2024

DR. SUDARSHAN KUMAR BABU VALLURU
(SUPERVISOR)

DR. VANJARI VENKATA RAMANA
(CO-SUPERVISOR)

ABSTRACT

This work presents the design and analysis of Zero-Current Switching Switched-Capacitor and Innovative Buck-Boost + Cuk Converter cell equalizing circuits for series-connected batteries. The study has two main objectives. The first objective is to develop a voltage equalizer for series batteries using a two-resonant state switched capacitor technique. Unlike traditional voltage equalizers, this approach does not require large magnetic components or a complicated monitoring and control mechanism. Switched-capacitor battery balancing circuits have potential among active balancing techniques due to their affordability, compact design, and simplicity. However, achieving full cell equalization with switched-capacitor equalizers is challenging and a higher voltage difference between cells reduces equalizing efficiency, while a smaller voltage difference slows down the balancing process. The proposed circuit improves on current switched-capacitor-based cell balancing circuits as its balancing speed is independent of the number of battery cells and the starting misfit of distribution of cell voltages. All switches in the stated equalizing circuit operate under zero-current switching. It can also be integrated with a bidirectional buck-boost converter for charging and discharging along with equalization. The second objective is toperform active cell balancing using a dc-dc converter—the Buck-Boost + Cuk converter for the battery cells connected in series. Traditionally, the buck-boost converter or the Cuk converter would be used to balance n battery cells in a battery pack that would require $(2n-1)$ switches. Nevertheless, by combining the buck-boost converter and the Cuk converter, the final buck-boost + Cuk converter requires only n switches. Unlike many previous one-switch-per-cell configurations, this design decreases the switch count by approximately half without sacrificing the benefits of modularization or raising device voltage stress. A SEPIC converter-based charger is also integrated in parallel with this topology to perform cell balancing and charging simultaneously. Both circuits can be controlled using just two complementary square-wave signals with a 50% duty cycle, similar to existing switched-capacitor-based cell balancing systems or buck-boost and Cuk converter-based battery charge equalizers. Simulation results show that the first architecture performs well in terms of equalization, achieving zero current switching and zero voltage gap between cells, whilethe second architecture provides zero voltage gap with a faster equalization. The designed systemoutcomes are validated using MATLAB-Simulink.

DEPARTMENT OF ELECTRICAL ENGINEERING
DELHI TECHNOLOGICAL UNIVERSITY
(Formerly Delhi College of Engineering)
Bawana Road, Delhi-110042

ACKNOWLEDGEMENT

I would like to extend my heartfelt gratitude to everyone who has generously contributed their valuable time and effort to assist me. Without their support, understanding, and guidance, completing this project would not have been possible.

I am deeply thankful to **Dr. Sudarshan Kumar Babu Valluru** (Professor, Department of Electrical Engineering, DTU, Delhi) and **Dr. Vanjari Venkata Ramana** (Assistant Professor, Department of Electrical Engineering, DTU, Delhi), my project guides, for their unwavering support, motivation, and encouragement throughout the duration of this project. Their constant readiness for consultation, insightful comments, and practical assistance have been invaluable to my work.

Lastly, I want to express my profound gratitude to my parents, seniors, and friends. Their unfailing support and continuous encouragement throughout my research work have been asource of immense strength and inspiration for me.

Date: 31/05/2024

Archit Chauhan
M. Tech (Power Electronics & Systems)
Roll No. 2K22/PES/05

TABLE OF CONTENTS

LIST OF FIGURES

LIST OF TABLES

LIST OF ABBREVIATIONS

EV	Electric Vehicle
HEV.	Hybrid Electric Vehicle
BMS	Battery Management System
SMPC	Switch Mode Power Converters
SC	Switched Capacitor
ZCS	Zero Current Switching
SPDT	Single Pole Double Throw
SOC	State of Charge
SOE	State of Energy
C-Rate	Charging/ Discharging Rate
LC	Inductor-Capacitor
EMI	Electro Magnetic Interference
CC	Constant Current
CV	Constant Voltage
ZVG	Zero Voltage Gap
ESR	Equivalent Series Resistance
OCV	Open Circuit Voltage
SEPIC	Single-Ended Primary-Inductor Converter
V2G	Vehicle 2 Grid
PWM	Pulse Width Modulation
MOSFET	Metal Oxide Semiconductor Field Effect Transistor

LIST OF SYMBOLS

B_n	n^{th} cell in top group
$B_{n'}$	n^{th} cell in bottom group
S_n	n^{th} switch in top group
$S_{n'}$	n^{th} switch in bottom group
V_{Bn}	Voltage of n^{th} cell in top group
$V_{Bn'}$	Voltage of n^{th} cell in bottom group
f_S	Switching frequency
f_r	Resonant frequency
L	Inductance in every RLC tank
C	Capacitance in every RLC tank
R	Parasitic resistance
R_{eq}	Equivalent resistance
i_{Cn}	Capacitor current of n^{th} cell in top group
$i_{Cn'}$	Capacitor current of n^{th} cell in bottom group
ω_r	Resonant angular frequency
V_L	Inductor voltage
V_C	Capacitor voltage
V_R	Resistance voltage
V_{B_min}	Minimum cell voltage
ΔV_{B_max}	Largest voltage difference between all the cells
V_{Cn_min}	Minimum voltage of n^{th} capacitor in top group
$V_{Cn'\_min}$	Minimum voltage of n^{th} capacitor in bottom group
V_{Cn_max}	Maximum voltage of n^{th} capacitor in top group
$V_{Cn'\_min}$	Maximum voltage of n^{th} capacitor in bottom group
ΔV_{Cn}	n^{th} capacitor ripple voltage in top group
$\Delta V_{Cn'}$	n^{th} capacitor ripple voltage in bottom group
Q	Quality factor
I_{Bn}	Current from n^{th} cell in top group
$I_{Bn'}$	Current from n^{th} cell in bottom group
V_S	DC voltage source in bi-directional charger circuit

C_{Bus}	Capacitance of bus used in bi-directional battery charger circuit
R_{Bus}	Resistance of bus used in bi-directional battery charger circuit
C_f	Capacitance of LC filter used in bi-directional battery charger circuit
L_f	Inductance of LC filter used in bi-directional battery charger circuit
R_L	Inductor resistance in bi-directional battery charger circuit
R_C	Capacitor resistance in bi-directional battery charger circuit
R_{Load}	Load resistance in bi-directional battery charger circuit
R_{ON}	On state resistance of MOSFET
C_{GS}	Gate to source capacitance of MOSFET
V_{Batt}	Battery voltage in bi-directional battery charger circuit
i_{Batt}	Battery charging in bi-directional battery charger circuit
V_{Batt*}	Reference battery voltage in bi-directional battery charger circuit
$I_{B\_Ref}.$	Reference battery charging current in bi-directional battery charger circuit
V_{Load*}	Reference load voltage in bi-directional battery charger circuit
V_{Load}	Load voltage in bi-directional battery charger circuit
Δv_c	Output voltage ripple in SEPIC battery charger circuit
$\Delta i_{L1}, \Delta i_{L2}$	Current ripple in inductors (L_1, L_2) in SEPIC battery charger circuit

CHAPTER 1
INTRODUCTION

1.1 BACKGROUND

The ecosystem has been greatly damaged by the widespread use of fossil fuels, which has led to resource depletion and global warming. In addition to using a lot of oil, traditional steam locomotives and other fossil fuel-powered cars release exhaust fumes that worsen the greenhouse effect [1]. As a result, energy saving and carbon reduction are becoming increasingly important on a global scale. In response, electricity-powered electric cars (EVs) have become a viable remedy and are anticipated to be a future trend in automotive design [2]. For high power battery applications like electric vehicles (EVs) and hybrid electric vehicles (HEVs), lithium-ion batteries are crucial due to their high density of energy, minimal self-discharge rate, and absence of memory effect [3]. To meet the power and energy requirements of EVs and HEVs, battery banks made up of hundreds of thousands of cells that are stacked in either parallel or series configuration must be built. This is because a single battery cell has a finite voltage and capacity [4].

For instance, the 7616 lithium-ion 18650 batteries used in the Tesla Model S are linked in parallel and series. The serial string charges and discharges collectively. The non-uniform individual cell characteristics of series cells cause a minor imbalance when they operate together, which shows up as uneven voltages between the cells throughout the charging and discharging phases [5]. Overcharging and deep draining the battery will both destroy the cell permanently or exacerbate it. The SOC graph of eight series-connected cells is displayed in Fig. 1.1, and it clearly illustrates how the SOC of different cells becomes unbalanced with time. There are two primary causes of this imbalance issue. First, manufacturing flaws in the cells result in differences in open circuit voltages (OCV), rate of discharging by themselves, ageing rates, and cell impedance values. Secondly, uneven heat management also causes different operating conditions in batteries; cells with higher state of charge (SOC) are therefore fully charged before those with lower SOC, and those with

lower SOC are prone to be completely discharged faster. Under certain conditions, this can lead to overcharging of some cells and a host of abnormal phenomena, such as premature aging, Li-plating, electrode structure disorganization, and possibly short circuits and flames [6].

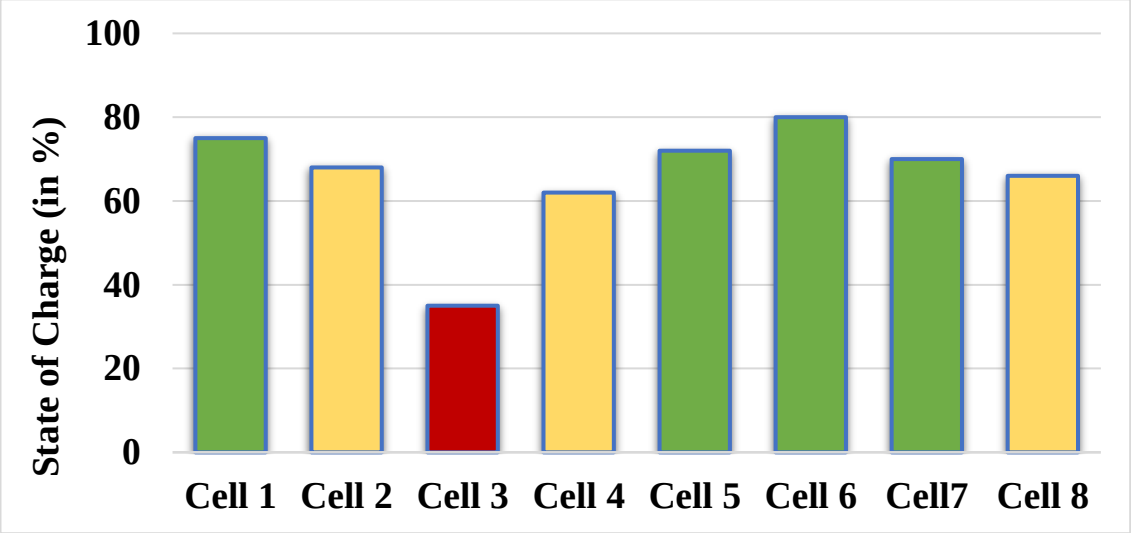

Fig. 1.1 Imbalance of cell SOC

The two scenarios are shown in Fig. 1.2; as can be observed, the SOC of each of the eight cells varies, indicating that the battery's initial condition is maintained in both circumstances. The two weakest cells overall with the lowest SOC are cells 4 and 6. Case 1 illustrates the battery module emptying. If the battery pack is allowed to empty, a single cell with subpar performance will be the only thing preventing the entire series string from operating regularly. In this instance, cell 4 depleted the battery pack most quickly and dictated its overall performance while the other cells were left unused. In case 2, the battery pack was left to charge in its initial condition. Over time, however, when other cells in the battery pack reached their charging limits, cells 4 and 6 continued to be undercharged. As a result, the battery performs worse and has a shorter lifespan due to this SOC imbalance. In actuality, enhancing the battery's chemistry might not be the best method to address this problem. To prevent cell imbalance, it also uses suitable power electronics topologies, which are also known as battery equalization.

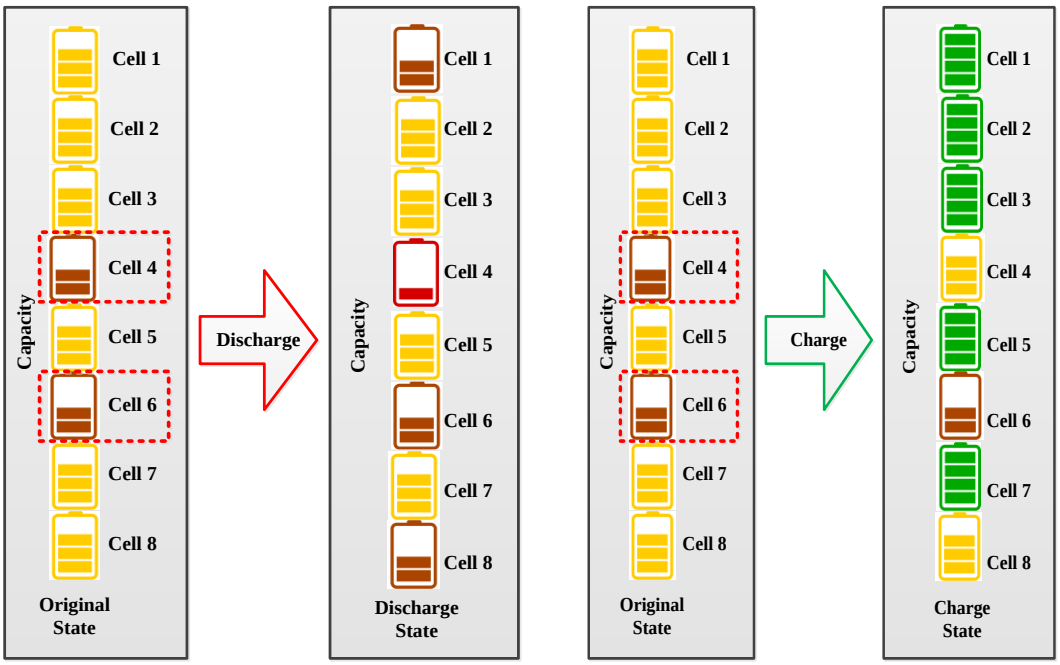

(a) Case 1 (b) Case 2

Fig. 1.2 Faulty cells determining battery pack performance

Numerous circuits and methods have been developed in for cell balancing. These balancing strategies fall into two divisions: active equalization and passive equalization [7]. These cell balancing topologies are depicted in Fig. 1.3. Another name for passive equalization is "resistor bleeding equalization." By using semiconductors to connect resistors in parallel with each cell, this method lowers excess voltage. These methods have the wonderful advantages of being portable, affordable, and easy to use. However, their primary shortcomings are related to heat control and energy dissipation. These issues are addressed by active cell balancing topologies, which transfer energy from the strong cells to the weak ones via non-dissipative energy-shuttling components. As a result, less energy is lost. Therefore, in terms of balancing capacity and efficiency, active balancing approaches perform better than passive equalization techniques. A method that relies on switched-mode power converters (SMPC) encompasses several types such as buck-boost, half-bridge, quasi-resonant LC, flyback, multi-winding transformers, and multiphase interleaved converters [8].

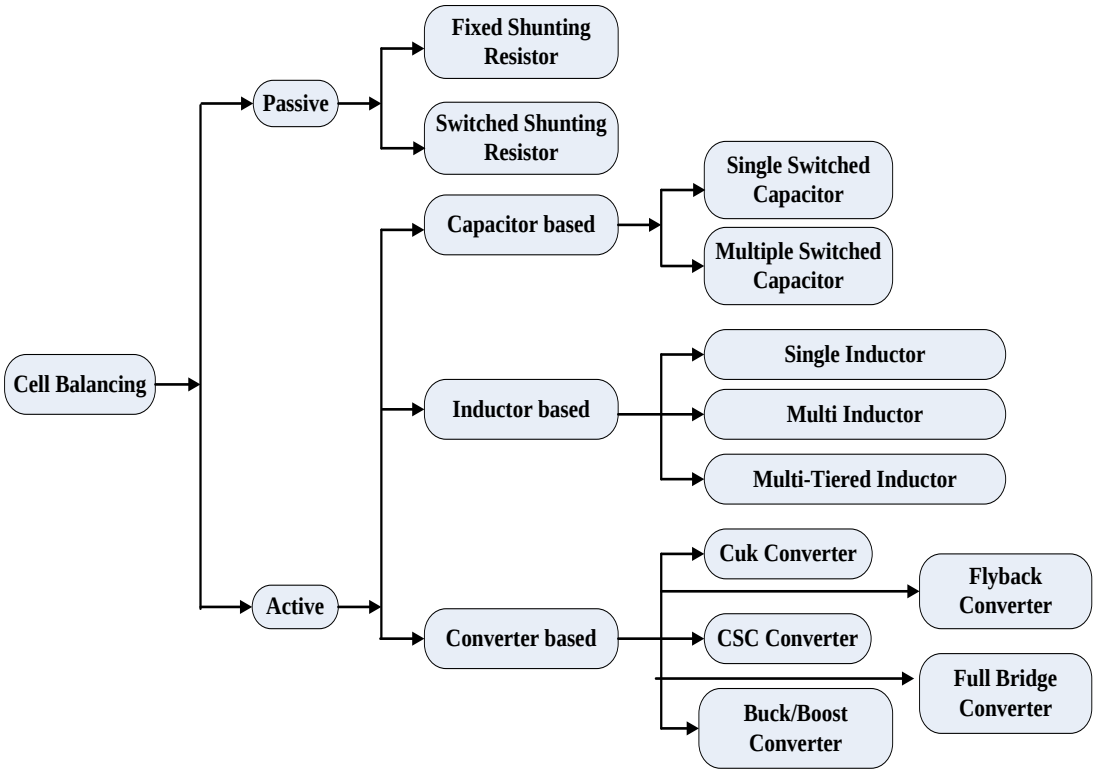

Fig. 1.3 Cell balancing topologies

multiphase interleaved converters.

Among the active balancing topologies with built-in benefits of reduced size, cheaper cost, simpler control, and increased efficiency are switched-capacitor (SC) based systems [9]. As the number of battery cells increases, the balancing effectiveness of the SC-based cell equalization circuits, such as ladder-type, double-tiered, and chain-structure circuits, continuously decreases [10]. A ladder-type SC equalization circuit allows for the movement of energy between two adjacent cells. The balancing speed reduces with an increase in the number of series-connected cells [11]. Moreover, hard switching can be found in the majority of SC-based cell equalization circuits. The current surge of capacitors during switching causes high switching loss and electromagnetic interference (EMI). Furthermore, a current surge in hard switching SC circuits will affect the component service life [12]. A resonant-based cell balancing technique is proposed in the literature to address this problem. It compels all switches to function with zero-current switching (ZCS) and suggests a SC equalization technique for battery packs connected in series. This technique

distributes charge across the two cells next to each other employing a single capacitor. By continuously flipping the capacitor back and forth, the unequal charge is dispersed until the two cell voltages are precisely equal. SC-based equalization just requires two complementary signals with a predetermined frequency and duty ratio. The lower voltage cells then receive the excess energy from the higher voltage cells. As a result, it has a better control strategy [13].

1.2 THESIS MOTIVATION

When it comes to replenishable energy storage systems and electric vehicles (EVs), battery management is essential to improving longevity, performance, and efficiency. Keeping series-connected battery cells' voltage balance constant is a constant struggle since imbalances can shorten battery life, diminish efficiency, and even pose a safety risk. Conventional passive balancing techniques, which release surplus energy as heat, are easy to use and reasonably priced, but they have poor efficiency and extra thermal management requirements. As a result, active cell balancing strategies that balance energy between cells are becoming more and more popular since they enhance system performance and efficiency as a whole.

Techniques for active balancing, which fit into three groups: converter-based, inductor-based, and capacitor-based, provide a number of benefits over passive approaches. Through the transfer of energy across cells with different state of charges (SOCs), these approaches optimize the distribution of energy within the battery pack. Even with their advantages, current active balancing techniques frequently have complicated circuitry and have energy conversion losses.

By investigating two cutting-edge active cell equalization topologies—the Buck-Boost + Cuk Converter and the Zero-Current Switching (ZCS) Switched-Capacitor approach—this thesis seeks to overcome these issues. By guaranteeing that all switches function under zero-current situations, lowering electromagnetic interference, and prolonging component lifespan, the ZCS Switched-Capacitor approach decreases energy losses. In the meantime, the Buck-Boost + Cuk Converter topology makes use of both converters' advantages to transfer energy efficiently with

fewer switches, which lowers component stress and circuit complexity. The project's objective is to create and evaluate these novel topologies in order to improve battery management systems' efficiency, dependability, and performance in electric vehicles (EVs) and other high-power applications. This initiative aims to enable the rising adoption of renewable energy resources and electric vehicles by resolving the shortcomings of existing balancing techniques and advancing energy storage technology. This thesis will show, via in-depth modeling and analysis, how the suggested approaches can effectively achieve superior cell balancing, enhancing battery performance and prolonging its operating life.

1.3 THESIS OBJECTIVE

The aim of this dissertation is to improve active cell balancing methods so that series-connected battery packs for electric cars and other high-power applications operate better and more efficiently. The study is focused on two main objectives, each of which addresses a particular difficulty with battery management and cell balancing.

The first objective is to design and build a switched-capacitor circuit with zero current switching (ZCS) that is integrated with a bi-directional buck-boost charging circuit. By using the resonant state switching capacitor technology instead of the huge magnetic components and intricate control mechanisms found in traditional voltage equalizers, this approach seeks to produce a voltage equalizer. By ensuring that all switches run at zero current, the ZCS approach greatly lowers electromagnetic interference switching losses and, prolonging the life of the battery's constituent parts. Incorporating a bi-directional buck-boost converter ensures equitable energy distribution across the cells by streamlining the charging and discharging process. The performance and efficacy of this topology are validated through the capture and analysis of charging and discharging waveforms.

The second objective is to create an alternative active cell balancing topology that equalizes more quickly than the ZCS Switched-Capacitor method by combining the Buck-Boost and Cuk Converter. This architecture minimizes component count and complexity while retaining excellent efficiency and reliability by reducing the number of switches needed. In order to accomplish simultaneous cell balancing and charging, a SEPIC converter-based battery charger is integrated with the Buck-Boost + Cuk scheme. This dual feature solves the problem of controlling different charging and discharging characteristics and aging in series-connected battery packs while also improving overall system efficiency. The speed, efficiency, and adaptability of the suggested system to changes in load and input circumstances are assessed.

When combined, these objectives seek to offer feasible methods to strengthen battery management systems and increase the efficiency, dependability, and longevity of batteries in high-power applications like electric cars. Detailed MATLAB-Simulink simulations demonstrating the efficacy of the suggested topologies validate the theoretical ideas and emphasize their real-world relevance.

1.4 THESIS ORGANIZATION

The whole design and control of two sophisticated active cell equalization topologies for battery banks connected in series are presented in this thesis, with an emphasis on applying cutting-edge methods to improve performance and efficiency. This thesis's outline is as follows:

Chapter 1: offers a succinct overview of the project, emphasizing the importance of environmental preservation and energy conservation in relation to electric cars (EVs). It talks about the difficulties caused by battery cell imbalance in lithium-ion battery packs that are connected in series and the need for successful cell equalization. Along with outlining the thesis's structure, this chapter also describes the thesis's goals and motivation.

Chapter 2: comprises a thorough literature review of the literature summarizing the most recent research on battery equalization methods. This chapter also sets the stage for the overview of the active cell balancing methods now in use. It discusses the benefits and drawbacks of several techniques, such as power converter-based balancing, inductor-based balancing, and switched-capacitor balancing and suggested remedies by pointing out the shortcomings and difficulties with the current approaches.

Chapter 3: examines the switched capacitor topology with Zero-Current Switching (ZCS) technology. The setup, computational modeling, and bi-directional charger circuit for battery pack charging and discharging are covered. The success of this strategy is demonstrated by the simulation results presented in this chapter, along with modes of operation.

Chapter 4: emphasizes the topology of the Buck-Boost + Cuk converter. Together with the integration of a battery charger circuit based on a SEPIC converter, it offers a thorough setup and mathematical analysis of the circuit. The faster equalization time achieved with this topology is highlighted, and the modes of operation and simulation results are also reviewed.

Chapter 5: outlines the full thesis and highlights the key findings and conclusions from the research. It describes the potential for further research in this area and analyzes the general efficacy of the suggested active cell balancing strategies.

CHAPTER 2
LITERATURE REVIEW

2.1 LITERATURE REVIEW

Modern electric vehicle (EV) propulsion systems count on lithium-ion (Li-ion) batteries due to their extended cycle life and high energy density. Nonetheless, imbalances within the battery pack may result from age, variations in cell capacity and inequalities in internal resistance [14]. If this imbalance persists, it may impair battery function, decrease usable capacity, and raise the possibility of safety issues. Li-ion battery longevity and optimal performance are therefore dependent on the use of active cell equalization methods in battery management systems (BMS).

Li-ion batteries can become imbalanced for a number of reasons, including as variations in self-discharge rates, temperature gradients during operation, and manufacturing variations. These variations can become noticeable as cells in a series arrangement charge and discharge, causing some cells to be overcharged and others to be undercharged. This imbalance may eventually cause a reduction in the total battery capacity and pose other safety hazards including thermal runaway [15].

It needs active cell balance to solve these problems. Active balancing enhances efficiency and reduces energy waste by shifting energy from higher-charged cells to lower-charged cells, unlike passive balancing, which expels excess energy in the form of heat [16]. This procedure guarantees that the battery pack functions within safe bounds while also extending the battery's lifespan.

The performance of various active cell equalization techniques has been explored in a number of research. One study uses hardware-in-the-loop validation to improve estimation algorithms and emphasizes the significance of preserving consistent state of charge (SOC) and state of energy (SOE) across battery cells. For efficient balance and overall battery management, accurate SOC and SOE calculation is essential. This ensures that energy redistribution is carried out exactly to prevent overcharging or deep draining any cell.

A thorough analysis of battery balancing techniques divided them into two groups: active and passive equalization. The effectiveness of active approaches in dispersing charge with minimal energy loss makes them the favored approach. These technologies include switched capacitor and inductor-based balancing. Among these, switching capacitor systems are especially well-known for their efficient ability to balance the voltage across batteries that are connected in series. These devices allow charge to go from cells with higher voltage to lower voltage ones by periodically connecting capacitors between the cells.

Using DC-DC converters is a possible novel option for active balancing. By altering the voltage as needed, converters such as the buck-boost and Cuk provide flexible balancing solutions. These converters are perfect for high-capacity battery packs where these imbalances are more noticeable since they can effectively handle significant voltage differentials between cells. To successfully balance the SOC, a buck-boost converter, for example, can distribute energy from a cell with higher voltage to a lower-voltage cell. Similar to this, a Cuk converter is a versatile tool for active balancing since it can perform both step-up (boost) and step-down (buck) adjustment.

To improve their performance, research has also looked into merging these converter topologies with other methods. In EV battery chargers, for instance, integrating active cell balancing with a SEPIC (Single-Ended Primary-Inductor Converter) design has demonstrated encouraging outcomes. Wide input voltage ranges and a non-inverted output are two benefits of SEPIC converters, which are essential for sustaining ideal charging conditions throughout the battery pack's cycle of different states of charge and discharge.

Additionally, in order to improve energy transfer efficiency and facilitate to-way power flow between the battery pack and the power grid, bi-directional battery chargers have been connected with active balancing systems. More adaptable and effective energy management is made possible by this integration, especially in vehicle-to-grid (V2G) applications where the battery of the car can serve as the grid's energy storage system [19]-[20].

In order to achieve active cell balancing, I concentrated on the ZCS switching capacitor and a buck-boost + Cuk converter architecture combination in this work. The great efficiency and low switching losses of the ZCS switched capacitor technology led to its selection. The balancing system's overall efficiency is improved by running in zero-current switching mode, which reduces energy wastage in the charge transfer process.

The integration of the buck-boost + Cuk converter topology allowed for greater voltage differential handling and offered a more adaptable balancing solution. A comprehensive solution for maintaining uniform SOC throughout the battery pack is provided by the Cuk converter, which provides the ability to execute both step-up and step-down conversions. The buck-boost converter efficiently regulates energy transfer between cells with considerable voltage changes.

Furthermore, these balancing systems enabled accurate control of the charging process through the integration of a battery charger based on a SEPIC converter. Irrespective of the battery cells' starting state of charge, the efficient and uniform charging of the cells was made possible by the SEPIC converter's wide input voltage range handling capabilities and steady, non-inverted output.

2.2 ACTIVE CELL EQUALIZATION

2.2.1 INTRODUCTION

Cell balancing is crucial to the maintenance of lithium-ion battery banks in order to guarantee maximum output, durability, and protection. Cell manufacturing variations, aging, and operating conditions can cause disparities in the capacity of the cell, internal impedance, and state of charge (SOC), resulting in imbalances where some cells charge or discharge more quickly than others [21]. Reduced useful capacity, increased aging, and possible safety hazards are the outcomes of these imbalances. As a result, efficient cell balancing strategies are essential, and active cell balancing has been shown to be an improved approach over passive balancing. The purpose of active cell equalization is to keep each cell within safe operating limits while maximizing the useful capacity of battery packs. Since the weakest cell in an imbalanced pack reaches its charge or discharge limits first, it decides the whole operation and longevity of the pack. In order to equalize the SOC across all cells, active cell balancing transfers energy from cells which have higher SOC to those with lower SOC. This procedure increases the battery's lifetime and efficiency in addition to increasing its total capacity. Although less complicated and costly, passive cell equalization is not as effective as active equalization. Higher SOC cells' excess energy is released as heat via resistors in passive equalization, which results in a major loss of energy, decreased efficiency, and possible problems with thermal management. Additionally, it is comparatively slow and loses effectiveness with increasing cell imbalances and battery aging [22]. One major disadvantage of passive balancing is that it wastes energy as heat, which makes it inappropriate for applications where battery longevity and energy efficiency are vital.

Active cell equalization has drawbacks despite its benefits. The main disadvantages are more complexity and expense as a result of the extra parts and control circuits needed. The battery management system's design and execution are made more difficult by the requirement for precise control mechanisms and sophisticated algorithms for efficient functioning. Furthermore, in small applications,

the physical space needed for these parts may be a limitation. The functioning of balancing circuits also results in higher parasitic losses, especially in transformer- and inductive-based systems. Even while these losses are far less than those caused by passive balancing, they nevertheless have an effect on the system's overall efficiency.

2.3 CAPACITIVE ACTIVE EQUALIZATION

Capacitors are used as energy storage devices in capacitor-based active balancing; they are usually coupled in parallel with battery cells. Cells which have a more state of charge (SOC) tend to transfer their surplus charge to those which have a low SOC using a technique called switched-capacitor equalization. Because of its basic control algorithms and easy implementation, it was among the first active balancing systems devised. Its balancing time can be very long, though, particularly if there are a lot of series-connected cells [23]. Many sophisticated circuits have been designed to enhance the efficiency and speed of balancing. These include mesh, double-tiered, chain, parallel, and delta structures. By offering more channels for the transmission of charges, these structures enhance overall performance in balancing.

2.3.1 Single Switched-Capacitor Equalization

Capacitors are used in single switched-capacitor equalization to balance the state of charge (SOC) of battery cells. This approach has the benefit of adaptable control algorithms, which makes it a workable solution for different battery setups. Every cell's SOC is tracked continually, and the balancing process initiates once the variation between the highest and lowest SOC exceeds a predetermined threshold. The initial stage in the procedure is to identify the cells with the greatest and the lowest SOC [24]. These two cells are connected to the capacitor via corresponding switches that are turned on. The excess energy is then moved from the cell with the greatest SOC to the cell with the lowest SOC via switches SPDT1 and SPDT2, which toggle at a particular frequency. This procedure continues until SOC of all the cells have a difference which is less than the threshold, signifying that the cells have

equalized. The main benefit of single switched-capacitor equalization is that, in cases where only two cells show appreciable SOC variances, it can balance quickly. This makes it possible to quickly redistribute energy regardless of where these cells are located inside the battery pack. However, since only two cells can be equalized in each cycle, the method's efficacy decreases when there is a significant variance in SOC across all cells. In certain situations, this restriction may lead to longer balancing times.

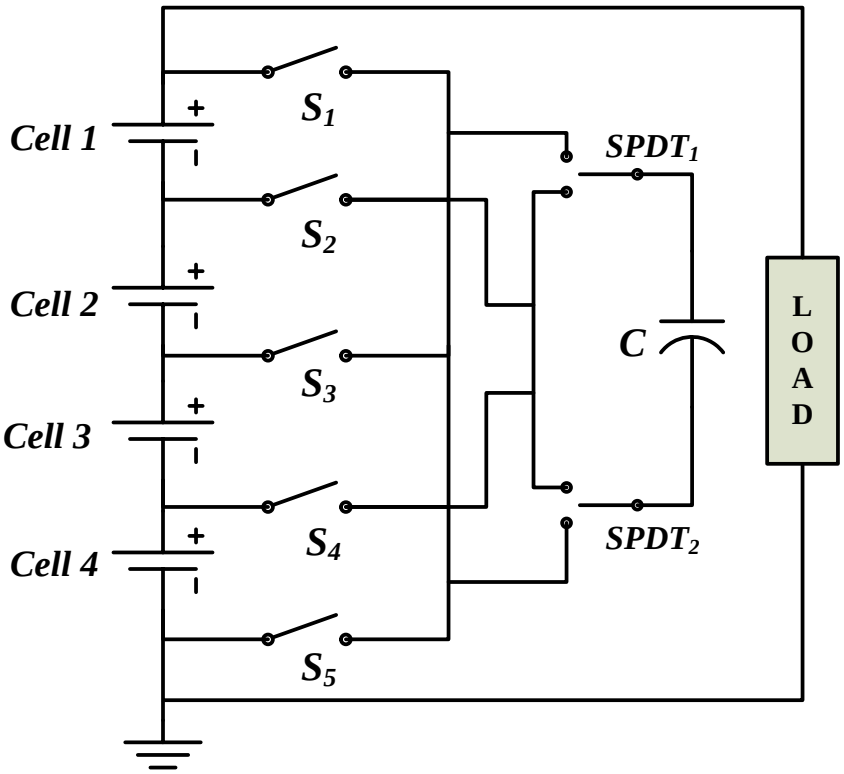

Fig. 2.1 Single switched capacitor equalization

2.3.2 Switched-Capacitor Equalization

With switched-capacitor equalization, a single-pole double-throw (SPDT) switch connects each capacitor across neighboring cells. All switches receive the same PWM impulses when the balancing mechanism is triggered, which causes them to toggle at the same frequency. With this configuration, each capacitor can connect

to two neighboring cells in turn, distributing excess energy from the cell with higher voltage to the lower-voltage cell. The advantage of switched-capacitor equalization is its ease of use. The control technique is simple and doesn't need comprehensive SOC data for every cell. This simplicity lowers the complexity of the control algorithms and facilitates system implementation [25].

But there are a lot of problems with this approach, especially when it comes to speed balance. There are two main reasons why the balancing time is longer. First, the voltage differential between neighboring cells gets smaller as the balancing process gets closer to its conclusion. Effective charge transfer across the capacitors is hampered by this tiny voltage differential. Secondly, within each balancing cycle, energy transfer in this system only takes place between nearby cells. Multiple balancing cycles are needed if surplus energy needs to be moved among distant cells in the series, which lengthens the overall balancing period.

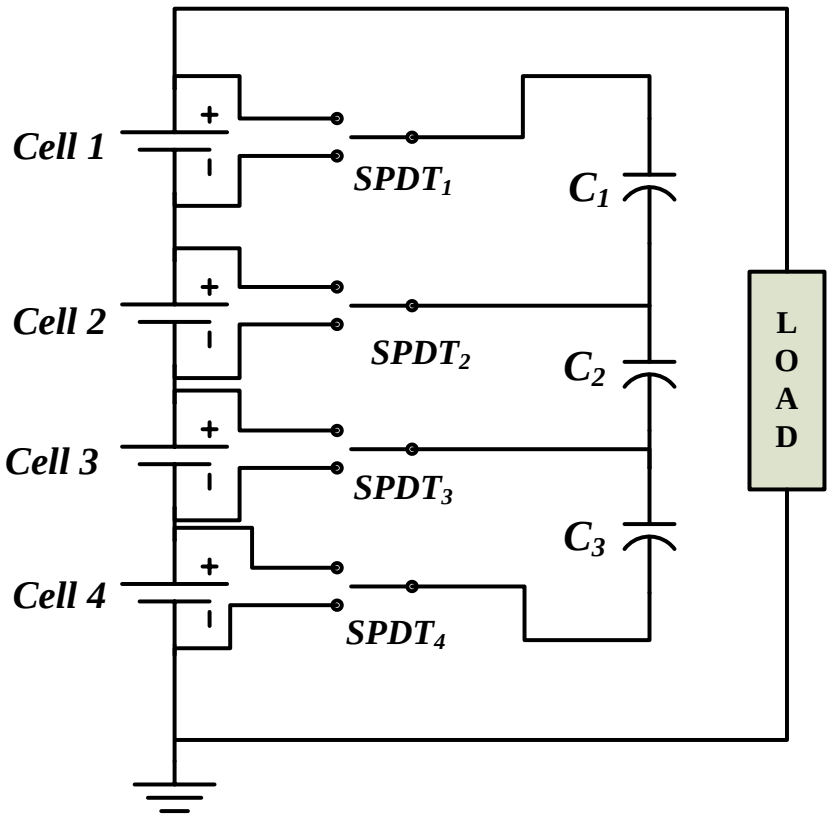

Fig. 2.2 Switched capacitor equalization

2.3.3 Double-Tiered Switched-Capacitor Equalization

Two layers of capacitors are used in double-tiered switched-capacitor balancing to increase efficiency and speed of balancing. Capacitors C_1, C_2, and C_3 make up the first layer in this arrangement, and capacitors C_4 and C_5 make up the second layer. Every switch toggle at the same frequency and receives the identical PWM signals, as shown in Fig. 2.3. The creation of charge-transfer shortcuts is this method's main benefit. For example, energy can move directly through C_4, bypassing C_1 and C_2, if there is a SOC imbalance between cell 1 and cell 3. By eliminating the need for as many energy conversion stages as possible, this direct transfer increases the efficiency and speed of balancing [26]. Nevertheless, there is a price for this enhanced performance. The balancing circuit's complexity and cost are increased by the requirement for extra capacitors in the second layer. The battery pack becomes larger physically as a result of this additional complexity, which may be a disadvantage in situations when space is at a premium. In general, double-tiered switched-capacitor balancing is faster and more cost-effective than single-layer switched-capacitor systems, but it also requires more complicated circuitry [27].

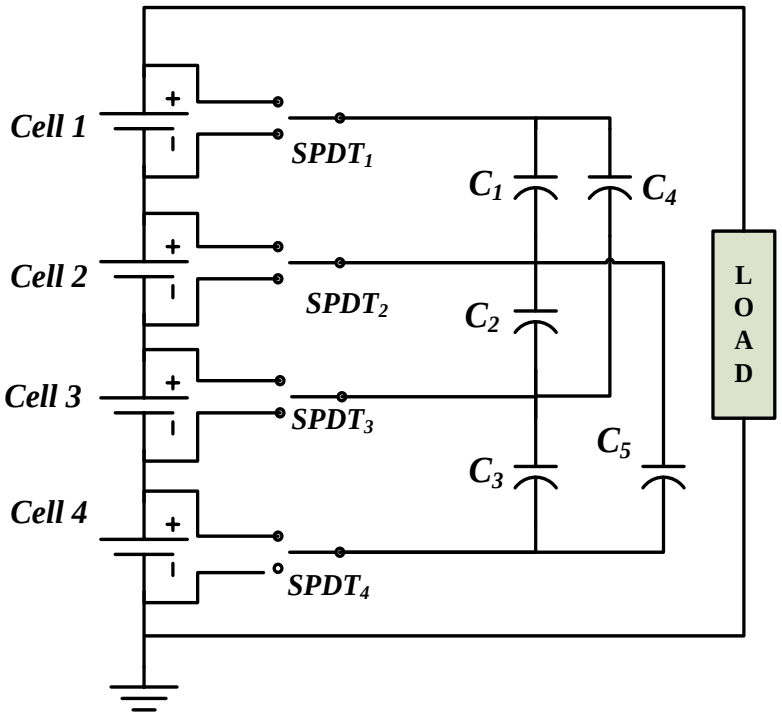

Fig. 2.3 Double tiered switched capacitor balancing

2.4 INDUCTIVE ACTIVE EQUALIZATION

Inductor-based active cell equalization functions by accumulating energy in the form of magnetic field as current passes through inductors. To attain balance, the stored energy can subsequently be divided among the cells. A range of topologies, including single inductor balancing, multi-tiered inductor balancing, multi-inductor balancing, and chain structure multi-inductor equalization, are possible depending on the count of inductors and switches used in the balancing circuits. Various configurations provide distinct benefits in terms of speed and efficiency, meeting varying demands for system complexity and equalization [28].

2.4.1 Single Inductor Equalization

With single inductor equalization, many MOSFETs are controlled by a single inductor to transmit extra energy. Depending on the way the energy is transferred, there are two categories for this technique. Energy is instantly distributed from the cell which has highest SOC to the cell with lowest SOC in the first type, which is quite similar to single switched-capacitor equalization. For example, when the cell 1 SOC is highest and that of cell 2 is lowest, then S_1 and S_2 are activated, permitting the current through inductor L to reach its maximum value. Subsequently, S_1 is switched off and S_5 is turned on, causing the inductor to discharge and sending surplus energy to cell 2. To prevent any potential short circuits, MOSFETs in the balancing circuits are coupled in series with diodes. The balancing speed is limited since only a couple of cells can be balanced every cycle. Despite this, accurate energy redistribution can be solved simply and effectively with single inductor balancing [29]-[30].

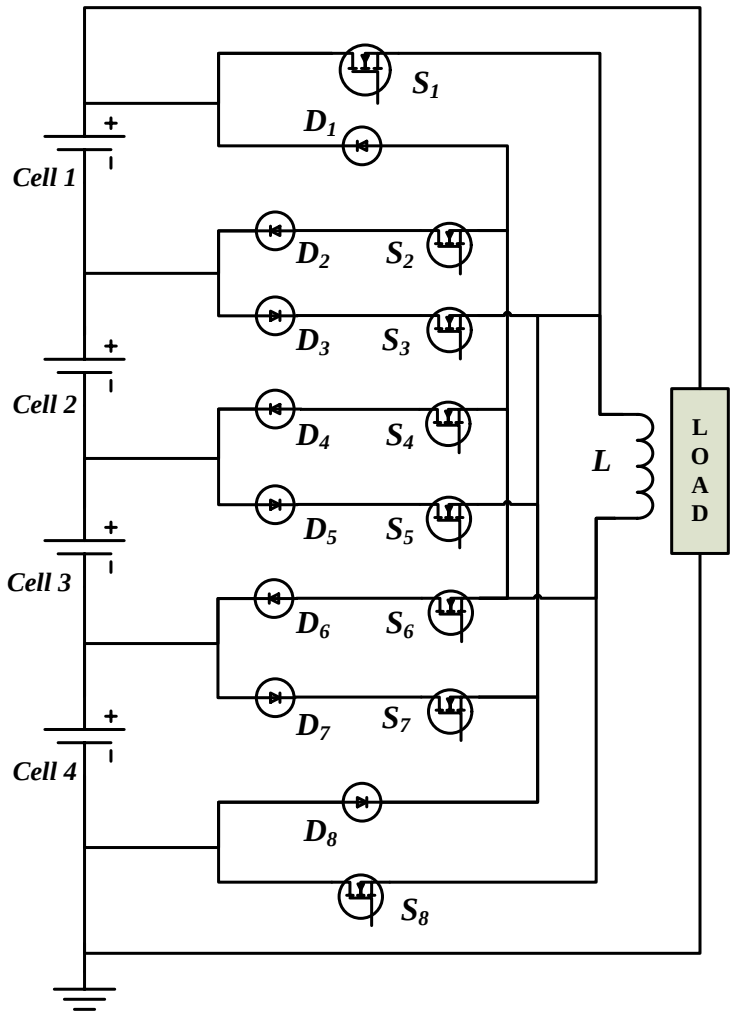

Fig. 2.4 Single inductor balancing

2.4.2 Multi Inductor Equalization

The aim of multi-inductor equalization is to balance several cell pairs at once. With this approach, every pair of neighboring cells has a separate inductor. MOSFET S_1 is activated while S_2 is kept off when balancing has to be done between cells 1 and 2, where cell 1 has a greater state of charge (SOC). As a result, inductor L_1 is charged and current rises. When S_1 is set to off position and S_2 is activated then the current in L_1 reaches its maximum value. This allows L_1 to discharge and transfer its stored energy to cell 2. Using inductors L_2, L_3, and so on, this procedure is repeated for the remaining pairs of cells to balance cell 2 with cell 3 and cell 3 with cell 4, correspondingly [31]. To decrease the SOC difference between adjacent cells, each

inductor helps transmit energy between the corresponding pair of cells. When opposed to single inductor approaches, multi-inductor balancing has the perk of being able to make numerous cell pairs at equilibrium concurrently, which can expedite the balancing process overall [32]. It is effective for balancing when the cells in series are in a large because of its synchronous balancing capacity.

However, this approach a major disadvantage of that it can only balance neighboring cells directly. Energy must be delivered successively through each cell and each inductor in between when there is a substantial SOC difference between the cells at dead ends of the series (for example, the first and last cells). Because of the numerous energy transformations involved in this step-by-step transfer, longer balancing times and higher energy losses result [33]. Multi-inductor balance is still a good choice in many situations when faster and more parallel balancing is needed, despite these disadvantages.

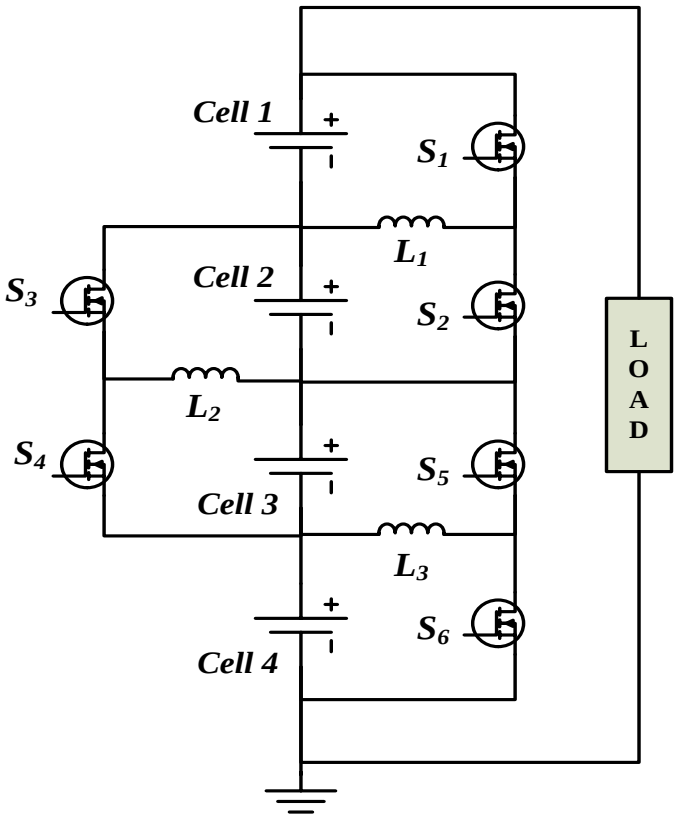

Fig. 2.5 Multi inductor balancing

2.4.3 Multi-Tiered Inductor Equalization

The efficiency of charge transmission between cells positioned at various positions within the battery pack is improved by multi-tiered inductor balancing. This method involves turning on a set of switches (S_1-S_7) while keeping the equivalent switches (S_8-S_{16}) off at first. Next, alternating cells are linked to inductors (L_1–L_7), and each inductor receives energy from its corresponding cell. The switches that are activated are then switched off, while the switches that are in the other direction remain inactive [34]. In the discharge phase, energy from inductors L_1–L_4 is sent through the internal diodes of (S_8–S_{11}) to cells in even-numbered slots, and energy from inductors L_5 and L_6 is sent through diodes of (S_{12} and S_{13}) to cells in odd-numbered slots. The highest-numbered cells in the series receive the energy that has been accumulated in inductor L_7 at this point.

Comparing this multi-tiered technique to older ways, the balancing procedure is completed faster because it generates seven different paths for charge transfer. However, the primary disadvantage of multi-tiered inductor balancing is the need for an increasing number of inductors as the series' cell count rises. This can result in larger physical footprints, more expensive circuits, and more complicated circuits—especially in applications using large battery packs [35]. Despite these difficulties, multi-tiered inductor balancing is a desirable alternative for situations requiring quick and accurate balancing of sizable battery arrays due to its increased efficiency and faster balancing speed.

2.5 CONVERTER BASED ACTIVE EQUALIZATION

The final category of active equalization techniques is converter-based active equalization. This method incorporates a number of different strategies, including quasi-resonant, flyback, Cuk, boost, and single converter balancing. To attain precise control over the charging and discharging processes within a battery pack, each kind makes use of distinct converter topologies [36].

Converter-based active balancing offers a very flexible and effective way to maintain balanced charge states among cells, which is crucial for maximizing performance and prolonging the lifespan of energy storage devices, despite its complexity and higher cost in comparison to alternative approaches.

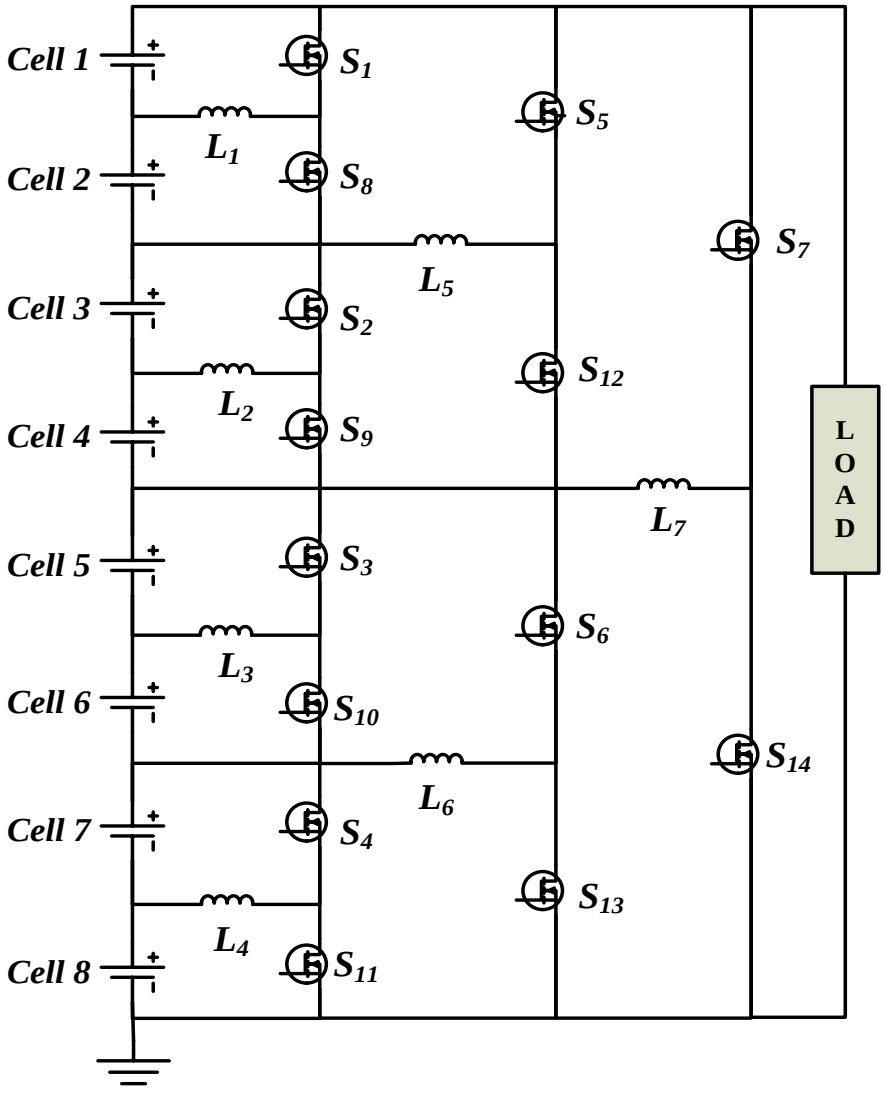

Fig. 2.6 Multi-tiered inductor balancing

2.5.1 Buck-Boost Converter Equalization

As demonstrated in Fig. 2.7, the buck-boost converter equalization circuit, uses the technique where a buck-boost converter is connected with a single cell to create a separate cell equalization block. The duty cycle of PWM signal delivered to the MOSFETs control the voltage conversion ratios and output power of these buck-boost converters. Buck-boost converter balancing provides more versatility by allowing the voltage conversion ratios to be both greater and lower than 1. This feature makes the control algorithms more flexible and allows for more accurate SOC management among the cells. The balancing procedure begins when the SOC difference between cells rises above a predetermined level. The MOSFETs are driven by PWM signals with the proper duty ratios; cells with higher SOCs receive signals that lower their voltage, and cells with lower SOCs receive signals that raise it. This modification promotes consistent SOC levels by ensuring effective energy transmission across cells [37].

However, to attain the same degree of flexibility and control, more complex electronics and control algorithms are needed. The battery management system's overall cost may go up if each cell requires its own buck-boost converter. Each additional component needed for a cell can result in a system that is bigger and possibly heavier.

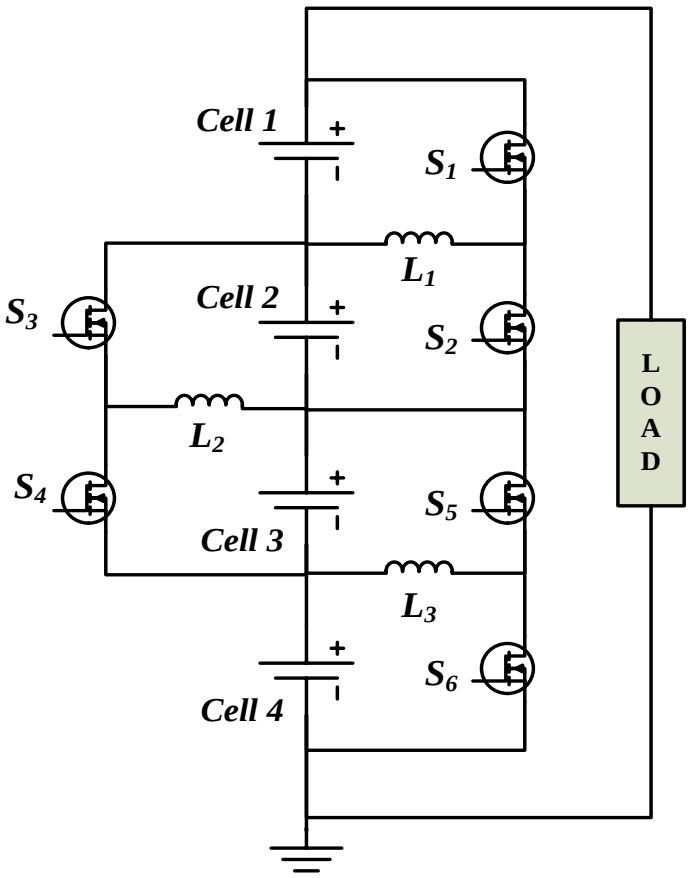

Fig. 2.7 Buck-boost converter equalization

2.5.2 Cuk Converter Equalization

Cuk converter equalization uses a Cuk converter between any two neighboring cells and works similarly to multi-inductor equalization, as shown in Fig. 2.8. The MOSFET S_1 operation in controlled to transfer energy from cell 1 to cell 2 if cell 1 has a greater SOC than cell 2. However, (N-1) Cuk converters are needed for a series connection of N cells, which raises the cost. Furthermore, it takes several energy conversion cycles and is slow to balance between non-adjacent cells. Although the approach is effective in lowering switching losses, two significant drawbacks are its high cost and delayed balancing for cells that are not nearby [38].

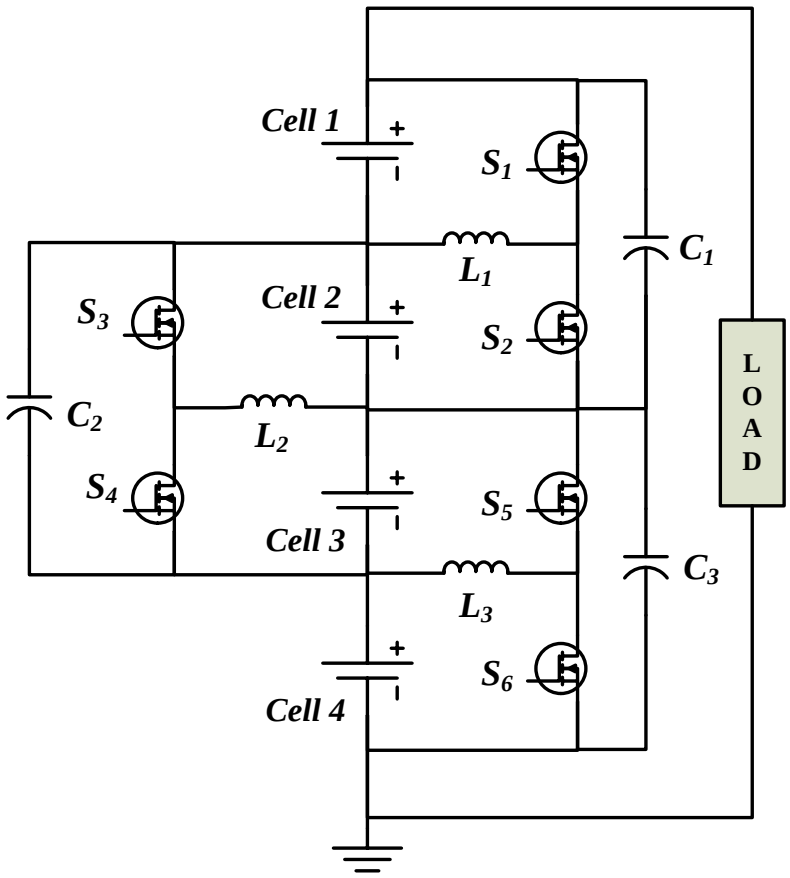

Fig. 3.8 Cuk converter equalization

2.5.3 Single Flyback Converter Equalization

Fig. 2.9 shows how single flyback converter balancing distributes energy among cells using a single transformer. Using this technique, cells with high SOC are identified and they are used to charge the whole battery pack via the transformer. PWM signals are transmitted to switches S_1 and S_2 when cell 1 has the excess energy than the other cells in series. When S_1 and S_2 are first activated, the transformer's current rises to its maximum level and energy is essentially distributed from cell 1 to the transformer. Diode D_0 blocks the flyback current during this period. The SOC of every cell is then balanced when S_1 and S_2 are shut off, allowing the transformer's stored energy to fly back and charge the whole battery. To safeguard the cells against potential short circuits, more diodes are included. The total cost of using a single

flyback converter is lower than that of using many converters. In comparison to adjacent-cell balancing techniques, the method balances the SOC between the whole battery pack and individual cells, resulting in a faster balancing speed [39].

But the control system, which involves transformer management and accurate PWM signals, can be intricate. The approach may not be as effective as other approaches in addressing small imbalances because it mainly concentrates on cells with noticeably greater SOC. By utilizing the effectiveness of transformer-based energy transfer, single flyback converter balancing provides a comparatively quick and affordable option for battery pack cell balancing.

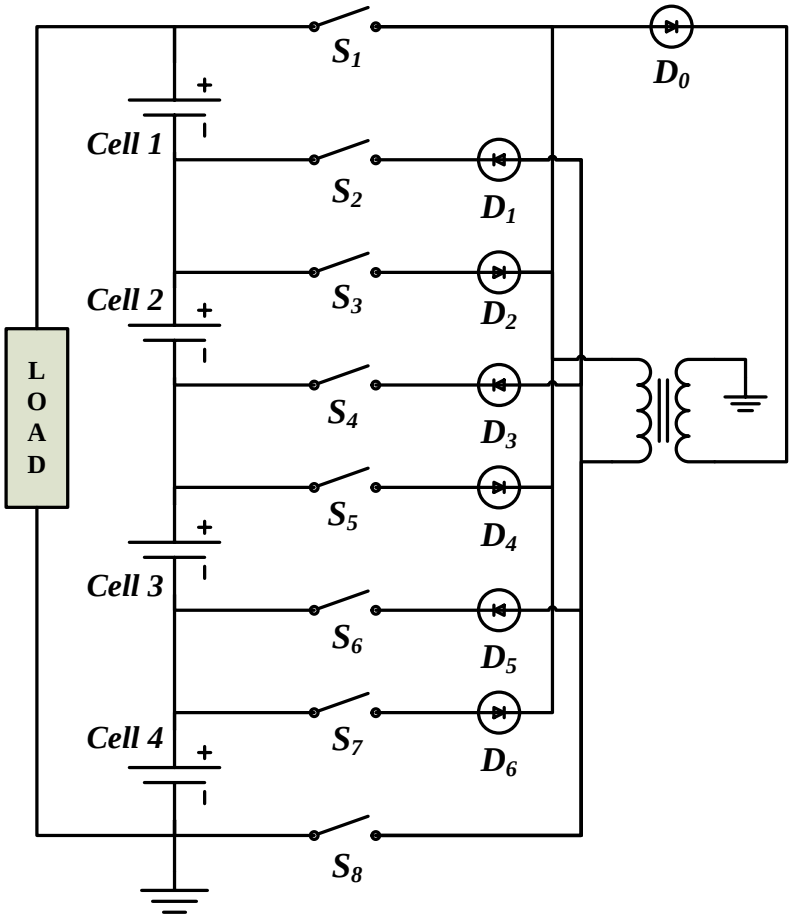

Fig. 2.9 Single flyback converter equalization

2.5.4 Multi Winding Flyback Converter Equalization

Multi winding flyback converter equalization technique can be used in two configurations, as shown in Fig. 2.10 and 2.11, to achieve successful cell balancing. In the very first configuration, individual cell is connected to a secondary winding, while the primary winding is connected to the entire battery. Both top and bottom balancing are supported in this configuration. When bottom balancing is used, the transformer receives power from the battery and distributes it to the cell which has the lowest SOC. On the opposite side, in top balancing, the transformer receives energy from the cell with highest SOC and returns it to the battery.

A more straightforward control algorithm is used in the second configuration. When switch S_0 is first activated, the transformer can be charged by the battery up until the current in the primary winding reaches its peak. After that, S_0 is disabled, allowing the transformer to supply energy to every cell. Due to the same turns on each secondary winding, cells with lower SOC (and hence lower voltage) receive bigger charging currents, whilst cells with higher SOC receive smaller currents, resulting in SOC levels that are balanced amongst cells. However, the secondary windings' variable leakage inductance limits this configuration's performance [40].

Effective balancing is made possible by the efficient energy transfer provided by both arrangements between the battery and the individual cells. The multiple winding architecture enables simultaneous balancing over several cells. On the other hand, balancing performance may be restricted by varying leakage inductances among secondary windings. The device's design becomes more complex and its size increases due to the requirement for a big magnetic core and many windings. Higher leakage inductance in large magnetic devices typically results in higher energy losses. All things considered, multi winding flyback converter balancing provides a flexible method of cell balancing; nonetheless, it faces difficulties with complex packaging and leakage inductance.

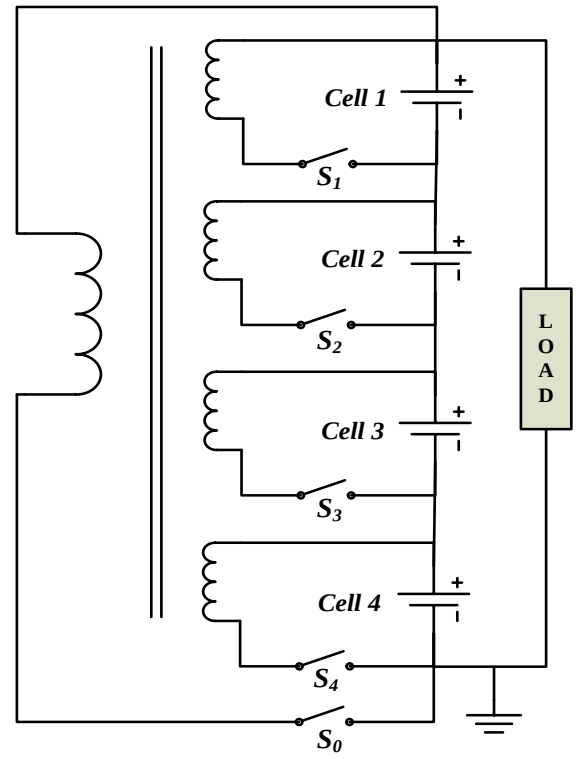

Fig. 3.10 Multi-winding flyback converter equalization (type 1)

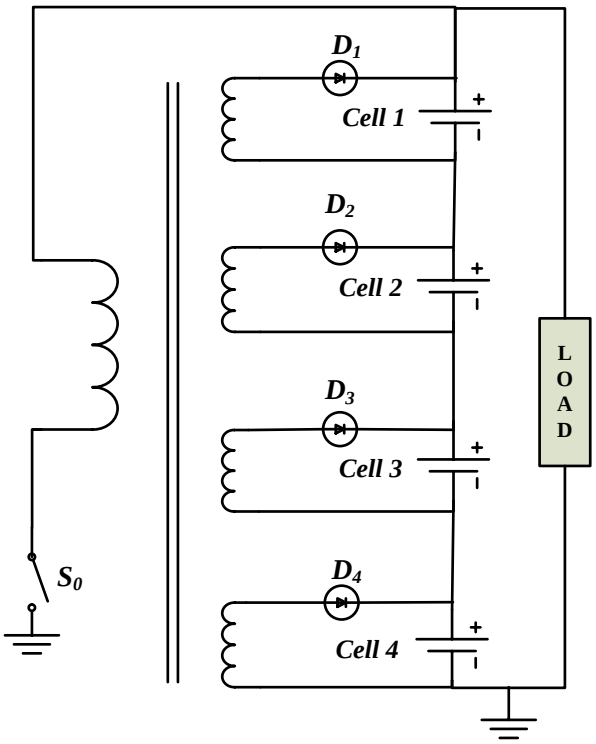

Fig. 3.11 Multi-winding flyback converter equalization (type 2)

2.6 CHAPTER SUMMARY

In the first section of the chapter, the importance of active cell equalization in battery management systems is discussed. Active cell equalization methods use components like capacitors, inductors, and converters to transfer energy among cells, improving overall efficiency and prolonging battery life, in contrast to passive balancing, which wastes surplus energy as heat. Even though it is more complicated and expensive, active balancing has a lot to offer in terms of keeping the State of Charge (SOC) constant between cells, which enhances battery longevity and performance.

By redistributing energy among battery cells, capacitors are used in capacitor-based active cell balancing to maintain a constant SOC. Energy is transferred from the cell with the highest SOC to the lowest SOC cell via single switched-capacitor equalization, which is effective for large SOC variances but less so for widely dispersed variations. It does this by using flexible control algorithms. With switched-capacitor balancing, capacitors are connected across each cell using SPDT switches. This allows for easy control over energy transfer between neighboring cells, but it requires longer balancing times, especially when voltage variations are small.

To equalize the SOC of cells, inductor-based active equalization uses inductors to store and distribute energy. The cells with highest and lowest SOC are connected by the employment of one inductor and several MOSFETs in single inductor balancing, which provides medium balancing speed with intricate control and effective handling of large SOC disparities. In order to balance neighboring cell pairs simultaneously, multi-inductor balancing uses numerous inductors. This method works well for nearby cells, but it takes longer to balance significant SOC differences and results in higher energy losses. Multiple layers of inductors are added in multi-tiered inductor balancing, which improves balancing time by providing multiple charge transfer channels. However, this method necessitates more inductors, which raises the size and expense of the system.

This section covers converter-based active balancing techniques, which renowned for their accuracy and adaptability. Boost converter equalization, however

more difficult and expensive, divides energy efficiently by altering the duty ratios of PWM signals and pairing each cell with a boost converter to create individual cell equalization units. Like boost converters, buck-boost converter balancing can modify voltage ratios above and below 1, providing more control at the expense of more expensive and intricate hardware. Cuk converter balancing connects neighboring cells and transfers energy with lower switching losses in the discontinuous capacitor voltage mode; however, it is less efficient for cells that are not nearby and necessitates a large number of converters. Single flyback converter balancing offers lower prices and faster balancing rates by charging the battery and balancing high SOC cells with a single transformer. However, additional protection diodes are required to prevent short circuits. In order to allow effective energy transfer in both bottom and top balancing modes, multi-winding flyback converter balancing uses a transformer with several secondary windings for each cell. However, leakage inductance and packing the big magnetic device are challenges.

CHAPTER 3
ZCS SWITCHED-CAPACITOR CELL BALANCING CIRCUIT

3.1 INTRODUCTION

The necessity for improved overall battery charging efficiency has been emphasized by recent developments in battery technology. This is because improved battery charging efficiency can directly reduce charging times and increase the longevity and performance of battery systems. This chapter explores the Zero-Current Switching (ZCS) Switched-Capacitor (SC) cell equalization circuit, a new approach intended to enhance the functionality of current SC cell balancing systems, in response to these needs. When combined with a bi-directional battery charger circuit, this approach is especially efficient and improves system simplicity while maintaining efficiency.

By getting away with the need for large magnetic components, the ZCS approach offers a significant benefit. It utilizes switches that function at zero current. This simplification makes the system more practical and economical by simplifying the entire design and minimizing the system's physical footprint. In addition, the ZCS SC cell balancing circuit's dependability and simplicity of use are increased because it doesn't require intricate monitoring and control systems.

This circuit's ability to maintain a steady balancing speed regardless of the how many battery cells are connected in the system or the initial imbalance in cell voltage distribution is one of its primary features. This guarantees consistent effectiveness and performance under a variety of operating circumstances. The bidirectional converter functions as a buck converter during the constant current-constant voltage (CC-CV) mode of charging and as a boost converter during the draining phase. It is managed by a sophisticated closed-loop Proportional-Integral (PI) controller. This double feature guarantees accurate control over the charging and discharging procedures as well as the best possible energy transfer.

Using MATLAB-Simulink, multiple simulations are carried out in order to validate the ZCS SC cell balancing circuit's efficiency and viability. These simulations show that the circuit can provide the intended system results, indicating

that it has the potential to greatly improve battery balancing and charging efficiency. Through tackling the primary obstacles linked to conventional balancing techniques, this study opens the door for more effective, dependable, and accessible battery management systems.

3.2 SYSTEM CONFIGURATION

The main drawbacks of conventional SC structures—their poor balancing speed and high switching losses—are addressed by the ZCS Switched-Capacitor (SC) cell equalization circuit. A SC-ZCS cell equalization circuit based on the resonance concept is shown in Fig. 3.1. With the addition of an inductor L, it has a resonant inductor-capacitor (LC) tank. Energy sharing between all series-connected n battery cells is facilitated by parallel connecting $(n-1)$ LC tank circuits with every pair of adjacent battery cells.

One capacitor, one inductor, and two switches make up this resonant loop; the total parasitic resistance is represented by R. Throughout the circuit, the capacitance (C) and inductance (L) values are constant. A single capacitor allows charges from neighbouring cells to interchange, alternating the distribution of charges until voltage parity is reached. The capacitance and resistance of the loop are negligible due to negligible internal resistances in the cells. Complementary square wave switching pulses control the ZCS function, allowing for effective energy transfer from the cells with higher voltage to lower voltage cells. This method reduces switching losses and balances cell voltage imbalances caused by battery chemistry, improving the battery system's overall longevity and performance.

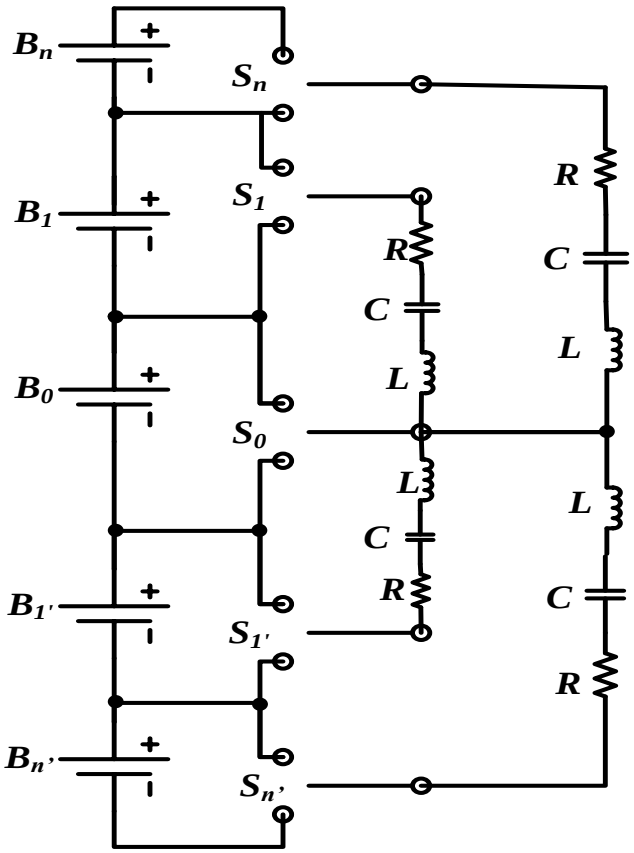

Fig. 3.1 ZCS cell equalization circuit

3.3 MATHEMATICAL ANALYSIS

There are basically two modes of operation for ZCS-SC cell equalization circuit.

In **State I** as illustrated in the Fig. 3.2 when the switches $\mathbf{S_n}$ & $\mathbf{S_0}$ connects the RLC tank from the top half of the circuit to cells $\mathbf{B_n}$ & $\mathbf{B_1}$, the capacitor current i_{Cn} gradually increase in a sinusoidal manner. Similarly, when the RLC tank from the bottom half connects to cells $\mathbf{B_{(n-1)'}}$ & $\mathbf{B_0}$ through corresponding switches $\mathbf{S_{n'}}$ & $\mathbf{S_0}$, capacitor current $i_{Cn'}$ rise in a similar manner.

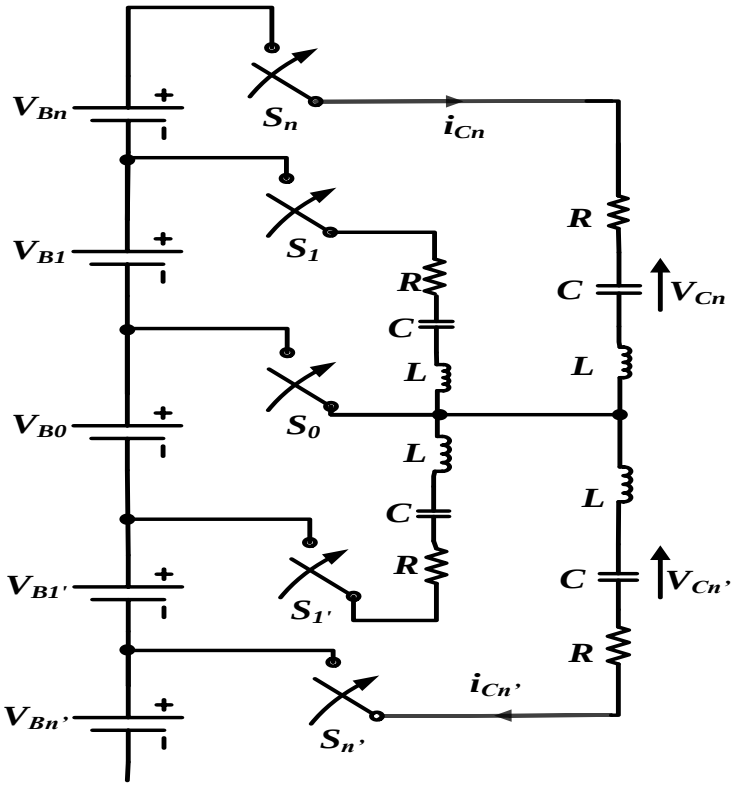

Fig. 4.2 Cell balancing circuit in state I

Taking one resonant loop in laplace domain,

$$I(s) = \frac{V_B/_s}{\left(sL + \frac{1}{sC} + R\right)} \tag{3.1}$$

Rearranging the terms,

$$I(s) = \frac{V_B}{L\left[\left(s + \frac{R}{2L}\right)^2 + \left\{\sqrt{\frac{1}{LC} - \left(\frac{R}{2L}\right)^2}\right\}^2\right]} \tag{3.2}$$

Substituting the values of ω_r and ρ as,

$$\omega_r = \sqrt{\frac{1}{LC} - \left(\frac{R}{2L}\right)^2} \text{ and } \rho = \frac{R}{2L} \tag{3.3}$$

$$I(s) = \frac{V_B * \omega_r}{\omega_r L\left[\left(s + \frac{R}{2L}\right)^2 + {\omega_r}^2\right]} \tag{3.4}$$

Taking inverse laplace transform we get,

$$i_c(t) = \frac{V_B}{\omega_r L} e^{-\rho t} \sin \omega_r t \tag{3.5}$$

If minimum voltage across capacitor was assumed to be V_{c_min} and not zero then,

$$i_c(t) = \frac{(V_B - V_{c\_min})}{\omega_r L} e^{-\rho t} \sin \omega_r t \tag{3.6}$$

Generalizing it for ***n*** cells we get,

$$i_{cn}(t) = \sum_{i=1}^{n} \frac{(V_{Bi} - V_{cn\_min})}{\omega_r L} e^{-\rho t} \sin \omega_r t \tag{3.7}$$

Similarly for bottom loops,

$$i_{cn'}(t) = \sum_{i=0}^{n-1} \frac{(V_{Bi'} - V_{cn'\_min})}{\omega_r L} e^{-\rho t} \sin \omega_r t \tag{3.8}$$

Now we know, $V_L = L\frac{di}{dt}$

$$V_L(t) = \frac{(V_B - V_{c\_min})}{\omega_r} [\{e^{-\rho t} \cos \omega_r t * \omega_r\} + \{e^{-\rho t} \sin \omega_r t * (-\rho)\}] \tag{3.9}$$

and

$$V_R(t) = R * i(t) = \frac{(V_B - V_{c\_min})}{\omega_r L} * R * e^{-\rho t} \sin \omega_r t \tag{3.10}$$

Multiplying and dividing by 2 and forming the expression of $\rho = \frac{R}{2L}$ we get,

$$V_R(t) = 2\frac{(V_B - V_{c\_min})}{\omega_r} * \beta * e^{-\rho t} \sin \omega_r t \tag{3.11}$$

also,

$$V_C = V_B - (V_L + V_R)$$

therefore,

$$V_C(t) = V_B - \frac{\left(V_B - V_{c\_min}\right)}{\omega_r} e^{-\rho t} * \left[\rho \sin \omega_r t + \omega_r \cos \omega_r t\right] \tag{3.12}$$

Generalizing it for ***n*** cells we get,

$$V_{Cn}(t) = \sum_{i=1}^{n} V_{Bi} - \sum_{i=1}^{n} \frac{\left(V_{Bi} - V_{cn\_min}\right)}{\omega_r} e^{-\rho t} \left[\rho \sin \omega_r t + \omega_r \cos \omega_r t\right] \tag{3.13}$$

Similarly for bottom loops,

$$V_{Cn'}(t) = \sum_{i=0}^{n-1} V_{Bi'} - \sum_{i=0}^{n-1} \frac{\left(V_{Bi'} - V_{cn'\_min}\right)}{\omega_r} e^{-\rho t} [\rho \sin \omega_r t + \omega_r \cos \omega_r t] \tag{3.14}$$

The capacitor currents $i_{cn}(t)$ and $i_{cn'}(t)$ return to zero when half of the resonant period is over at $t = {}^{\pi}/_{\omega_r}$, and the switches turn OFF in accordance with ZCS condition.

At this time period all the capacitor charges up to their maximum voltage value given by V_{Cn_max} and $V_{Cn'\_max}$, *i.e.*,

$$V_{Cn\_max} = \left(1 + e^{-\rho\pi/\omega_r}\right) \sum_{i=1}^{n} V_{Bi} - V_{Cn\_min} e^{-\rho\pi/\omega_r} \tag{3.15}$$

$$V_{Cn'\_max} = \left(1 + e^{-\rho\pi/\omega_r}\right) \sum_{i=0}^{n-1} V_{Bi'} - V_{Cn'\_min} e^{-\rho\pi/\omega_r} \tag{3.16}$$

In **State II** as shown in the Fig. 4.3 the capacitor currents $\boldsymbol{i_{Cn}}$ and $\boldsymbol{i_{Cn'}}$ rise again in sinusoidal manner from zero, but in opposite direction when the RLC tank in top half of the circuit completes its connection in parallel to the cell $\mathbf{B_0}$ & $\mathbf{B_{n-1}}$ through corresponding switches $\mathbf{S_0}$ & $\mathbf{S_n}$**.** Similarly, the switches $\mathbf{S_0}$ & $\mathbf{S_n}$' in bottom half connects RLC tank to cells $\mathbf{B_1}$' & $\mathbf{B_n}$' respectively.

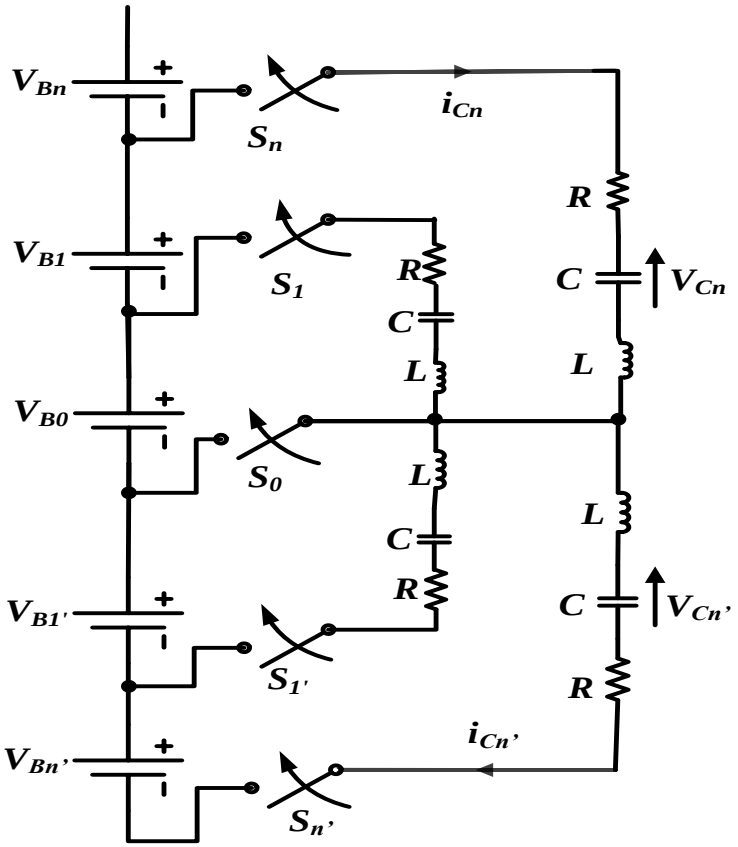

Fig. 3.3 Cell balancing circuit in state II

Equations of capacitor current and voltage remains same except the limits of summation.

$$i_{cn}(t) = \sum_{i=0}^{n-1} \frac{(V_{Bi} - V_{cn\_max})}{\omega_r L} e^{-\rho t} \sin \omega_r t \tag{3.17}$$

$$i_{cn'}(t) = \sum_{i=1}^{n} \frac{(V_{Bi'} - V_{cn'\_max})}{\omega_r L} e^{-\rho t} \sin \omega_r t \tag{3.18}$$

$$V_{Cn}(t) = \sum_{i=0}^{n-1} V_{Bi} - \sum_{i=0}^{n-1} \frac{(V_{Bi} - V_{cn\_max})}{\omega_r} e^{-\rho t} * [\rho \sin \omega_r t + \omega_r \cos \omega_r t] \tag{3.19}$$

$$V_{Cn'}(t) = \sum_{i=1}^{n} V_{Bi'} - \sum_{i=1}^{n} \frac{(V_{Bi'} - V_{cn'\_max})}{\omega_r} e^{-\rho t} * [\rho \sin \omega_r t + \omega_r \cos \omega_r t] \tag{3.20}$$

The capacitor currents $i_{cn}(t)$ and $i_{cn'}(t)$ return to zero when the resonant period gets over, at $t = {}^{2\pi}/_{\omega_r}$

The voltages of capacitors in both top and bottom tank reach to their minimum values V_{Cn_min} and $V_{Cn'\_min}$, i.e.,

$$V_{Cn\_min} = \left(1 + e^{-\rho\pi/\omega_r}\right) \sum_{i=0}^{n-1} V_{Bi} - V_{Cn\_max} e^{-\rho\pi/\omega_r} \tag{3.21}$$

$$V_{Cn'\_min} = \left(1 + e^{-\rho\pi/\omega_r}\right) \sum_{i=1}^{n} V_{Bi'} - V_{Cn'\_max} e^{-\rho\pi/\omega_r} \tag{3.22}$$

Voltage ripple ΔV_{Cn} is given by,

$$\Delta V_{Cn} = V_{Cn\_max} - V_{Cn\_min}$$

From Eq. (4.15) and (4.21)

$$\Delta V_{Cn} = \left(1 + e^{-\rho\pi/\omega_r}\right)\left(\sum_{i=1}^{n} V_{Bi} - \sum_{i=0}^{n-1} V_{Bi}\right) + e^{-\rho\pi/\omega_r}\left(V_{Cn\_max} - V_{Cn\_min}\right)$$

$$\Delta V_{Cn} - \Delta V_{Cn} e^{-\rho\pi/\omega_r} = \left(1 + e^{-\rho\pi/\omega_r}\right)(V_{Bn} - V_{B0})$$

Finally, the expression becomes

$$\Delta V_{Cn} = \frac{\left(1 + e^{-\rho\pi/\omega_r}\right)}{\left(1 - e^{-\rho\pi/\omega_r}\right)}(V_{Bn} - V_{B0}) \tag{3.23}$$

Similarly,

$$\Delta V_{Cn'} = \frac{\left(1 + e^{-\rho\pi/\omega_r}\right)}{\left(1 - e^{-\rho\pi/\omega_r}\right)}(V_{B0} - V_{Bn'}) \tag{3.24}$$

Assuming an RLC tank from the top half, the quantity of charge that travels from battery cell B_0 via B_n during one switching cycle, will be

$$Q = C * \Delta V_{Cn}$$

Therefore, the average current during one switching cycle flowing from B_n to B_0 is given by,

$$I_{Bn} = f_s * C * \Delta V_{Cn} \tag{3.25}$$

Similarly,

$$I_{Bn'} = f_s * C * \Delta V_{Cn'} \tag{3.26}$$

Substituting the values of ΔV_{Cn} & $\Delta V_{Cn'}$ we get,

$$I_{Bn} = f_s * C * \frac{\left(1 + e^{-\rho\pi/\omega_r}\right)}{\left(1 - e^{-\rho\pi/\omega_r}\right)}(V_{Bn} - V_{B0}) \tag{3.27}$$

$$I_{Bn'} = f_s * C * \frac{\left(1 + e^{-\rho\pi/\omega_r}\right)}{\left(1 - e^{-\rho\pi/\omega_r}\right)}(V_{B0} - V_{Bn'}) \tag{3.28}$$

The expression further reduces to,

$$I_{Bn} = \frac{(V_{Bn} - V_{B0})}{R_{eq}} \;\&\; I_{Bn'} = \frac{(V_{B0} - V_{Bn'})}{R_{eq}}$$

Where,

$$R_{eq} = \frac{\left(1 - e^{-\rho\pi/\omega_r}\right)}{C\, f_s(1 + e^{-\rho\pi/\omega_r})}$$

It is demonstrated that energy can be distributed between any two cells having a charge imbalance in just two steps. The current will go from the cells with higher voltage to central cell B_0 where they will subsequently enter the cells with lower voltage.

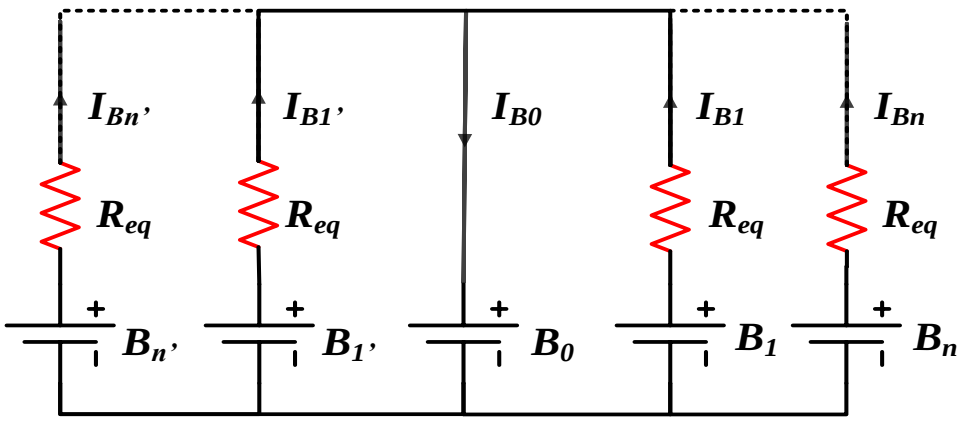

Fig. 3.4 Equivalent circuit of the above SC balancing circuit

We know that,

$$\tanh x = \frac{(1 - e^{-2x})}{(1 + e^{-2x})}$$

Expressing ωr & ρ in terms of quality factor Q

$$\sqrt{4Q^2 - 1} = \frac{1}{\beta}\sqrt{\frac{1}{LC} - \beta^2} = \frac{\omega_r}{\beta}$$

Rewriting the expression of R_{eq} in terms of quality factor Q, total parasitic resistance R, switching frequency f_s and resonant frequency f_r we get,

$$R_{eq} = \frac{2\,\rho\,Q^2 R}{f_s} * \tanh\left(\frac{\pi}{2\sqrt{4Q^2 - 1}}\right)$$

Taking R in denominator the final expression becomes,

$$\frac{R_{eq}}{R} = 4\pi * \frac{f_r}{f_s} * \frac{Q^2}{\sqrt{4Q^2 - 1}} * \tanh\left(\frac{\pi}{2\sqrt{4Q^2 - 1}}\right)$$

This represents the corresponding resistance ratio in terms of switching frequency f_s, resonant frequency f_r, quality factor Q.

When the graph of $\frac{R_{eq}}{R}$ is plotted against quality factor Q, then certain things get cleared regarding the values of various parameters to be kept in simulation circuit.

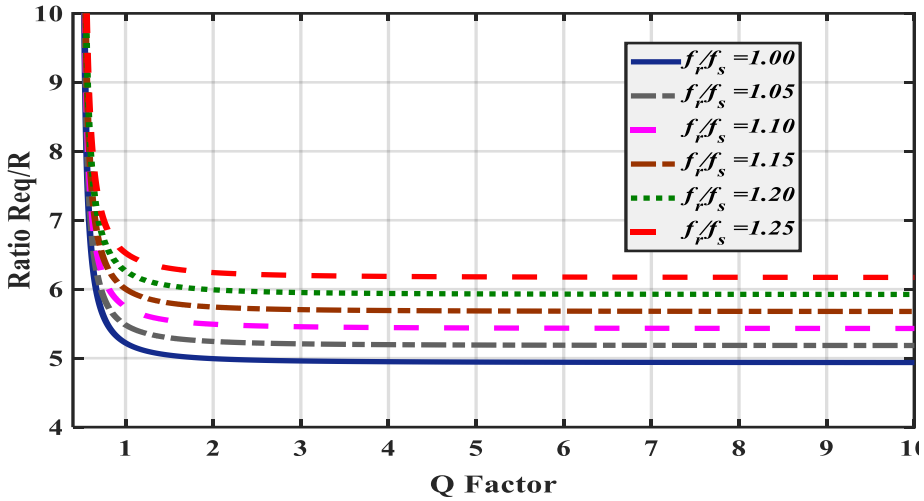

Fig. 3.5 Graph of the ratio $\frac{R_{eq}}{R}$ versus the Q factor.

These curves tell us that there is a major drawback when $Q < 1$because at that time the ratio $\frac{R_{eq}}{R}$ increases sharply and that is not desirable. However, this negative influence disappears when its value increases to be greater than 1.5. So quality factor must be greater than 1.5 somehow. To reduce the equivalent resistance and subsequently losses, all component parasitic resistances should be as little as feasible. After that, the frequency of switching ought to be nearer to the resonant frequency because a wider gap between the two will eventually lead to a higher $\frac{R_{eq}}{R}$ ratio and additional losses in the system.

3.4 BI-DIRECTIONAL BATTERY CHARGER CIRCUIT

A versatile circuit made to effectively control a battery pack's charging and discharging operations is the bi-directional battery charger circuit. The smooth transition between two operating modes made possible by this circuit architecture guarantees optimal performance during energy storage and distribution. It makes use of a bi-directional DC-DC converter, which, depending on the demands of the connected load and battery condition, operates as either a buck or boost converter and is essential to preserving battery health and efficiency.

The bi-directional DC-DC converter, as depicted in Fig. 3.6, consists of two complementary MOSFET switches, S_1 and S_2, a DC voltage source, V_S, and a bus capacitor, C_{Bus} with parasitic resistance, R_{Bus}. These switches manage the flow of energy and are linked to an LC filter, which is made up of an LC filter capacitor C_f and an inductor L_f with corresponding parasitic resistances R_L and R_C. Effective energy management is made possible by the battery pack's parallel connection to the filter, which serves as the goal for charging or discharging.

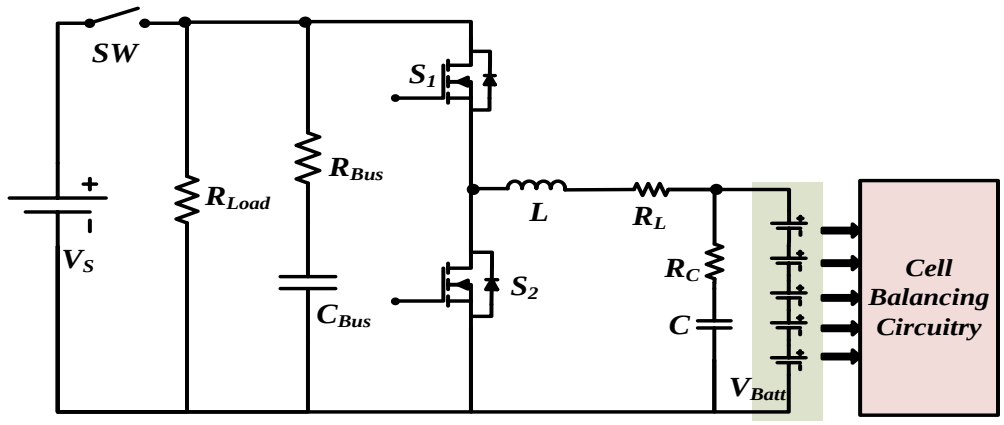

Fig. 3.6 Bi-directional battery charger circuit

The bi-directional converter has basically two modes of operation:

1) **Mode I (Buck Converter Mode)**

   As seen in Fig. 3.7 (a), the converter operates as a buck converter in this mode. The inductor L exhibits a linear rise in current flow when the input voltage V_S is applied across it. The output current i_{Batt} remains constant during this operation. Switch S_1 is activated while switch S_2 is disabled during this process, enabling the battery pack and load R_{Load} to charge.

2) **Mode II (Boost Converter Mode)**

   When the boost converter mode is engaged, current flows to the load and is supplied by the battery pack discharging through the inductor. To accomplish this, flip switch S_1 OFF and switch S_2 ON. In order to simulate the operation of a boost converter, the inductor L releases the stored energy to the load. Fig. 3.7 (b) shows an illustration of this mode.

The bi-directional battery charger maintains the health and functionality of the battery pack while ensuring effective energy transfer by alternating between these two modes. This allows it to accommodate different charging and discharging demands.

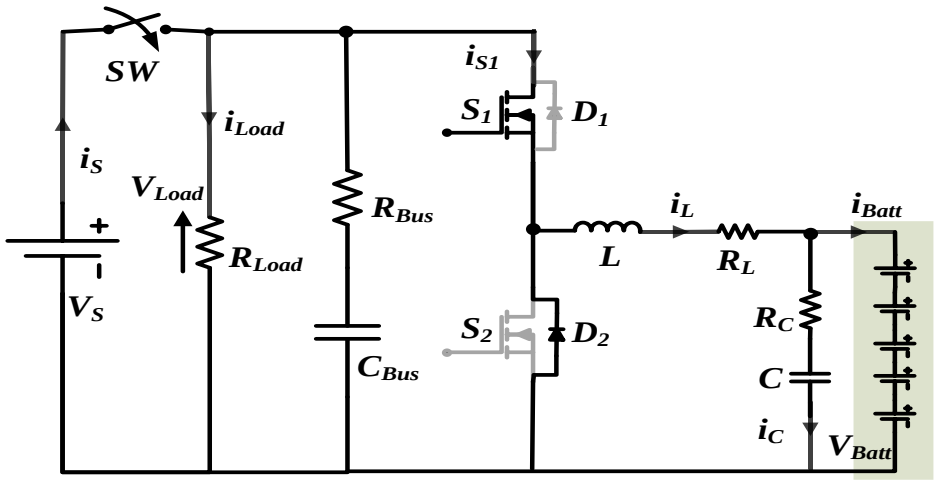

(a)

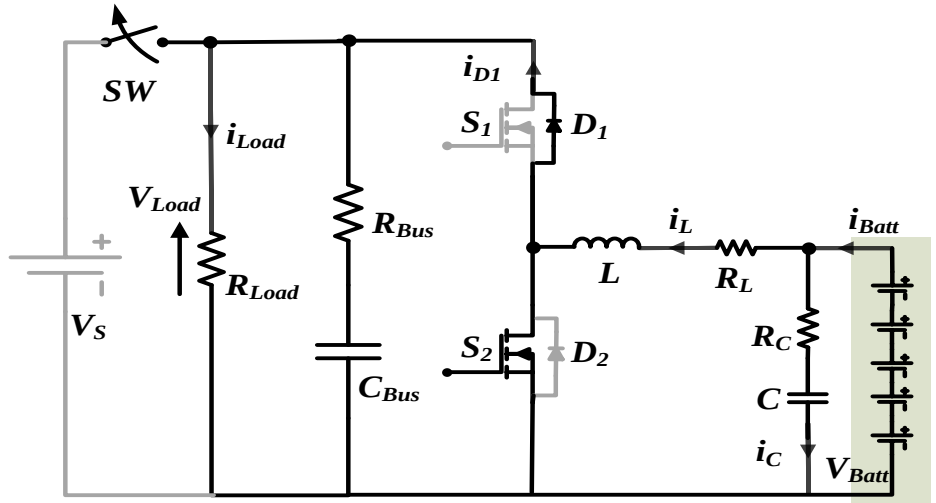

(b)

Fig. 3.7 Charger circuit modes of operation. (a) Mode I (b) Mode II

3.5 DESIGN AND CONTROL

To reduce the overall parasitic resistance R and thus losses, MOSFET on-state resistance (R_{ON}) should be as little as practical. Conversely, the MOSFET's gate-to-source is inversely correlated with the on-state resistance. This implies that a smaller R_{ON} leads to a greater C_{GS}, which raises the gate driving losses to some extent. Therefore, the R_{ON} cannot be very low. There is a trade-off between the switching

frequency and the on-state resistance of MOSFET since, a higher switching frequency is required to reduce the ratio $\frac{R_{eq}}{R}$, but doing so would increase the gate driving losses. Keeping in mind the curves from Fig. 3.5, the equivalent resistance R_{eq} value should be chosen to be approximately 5–6 times the total parasitic resistance, as this is the lowest ratio that will minimize the losses.

In this circuit for cell balancing, the capacitors to be used is always one less than the total number of battery cells utilized. The maximum voltage stress that the capacitors can tolerate is represented as $n \times V_{B\_max}$, where n represents the number of battery cells. The value of each capacitor in the top and bottom RLC tank capacitance C must satisfy the following requirement and be the same.

$$\frac{\Delta V_{C\_max}}{2} = \frac{\Delta V_{B\_max}}{2CR_{eq}f_s} < V_{B\_min}$$

Where, $V_{B_min}$is the voltage of the cell with lowest value among all series connected cells, ΔV_{B_max} is the largest voltage differential between all the cells in the battery pack and ΔV_{C_max} is the highest voltage ripple across the capacitor.

Inductors used in all RLC tanks should have the same value, just like capacitors, to guarantee that the resonant frequency stays constant throughout each loop. As shown in Fig. 3.5, when *Q* factor is more than 1.5, the ratio of $\frac{R_{eq}}{R}$ stays constant across a broad range. This suggests that the circuit's inductors simply have to be big enough to make certain that the *Q* factor is more than 1.5

Parameter	Value
Switching frequency (f_s)	50KHz
Resonant frequency (f_r)	50KHz
MOSFET on state resistance (R_{ON})	0.96mΩ
Tank capacitance (C)	10μF
Tank inductance (L)	1μH
Tank resistance (R)	0.18Ω
Quality factor (Q)	1.756

Table 3.1: Design Specifications of ZCS circuit

The circuit for the bi-directional battery charger is designed with two purposes in mind: to effectively control the charging and draining of a battery pack. When the system is in charging mode, the design methodology is similar to that of a conventional buck converter. This is because of the fact that, analogous to how a buck converter functions, the circuit reduces the input voltage while charging to a level appropriate for the battery.

Real-world component parasitic resistances are incorporated into the design to guarantee the circuit's practicality and dependability. These resistances consist of the parasitic resistance of the LC filter's inductor R_L and capacitor R_C, as well as the parasitic resistance of the bus capacitor R_{Bus}. To build a precise model and attain optimal performance, it is imperative to recognize these resistances.

Another crucial component of the design is the inductor's ability to work in the continuous conduction mode (CCM). Because it makes converter analysis and control easier, CCM is recommended. Since the inductor current never zeroes in this mode, the energy transfer mechanism is steadier and more effective.

To determine the appropriate inductor value for the circuit, the following formula is used:

$$L_{min} = \frac{(1-D)(R)}{2f} = 4.5 \text{ mH}$$

With the aim that the inductor operates in continuous conduction mode (CCM) mode, the inductor value is set to be 28% greater than the minimum.

$$L = 1.28\, L_{min} = (1.28)(4.5 \text{ mH}) = 5.76 \text{ mH}$$

Output capacitor value is found as,

$$C = \frac{(1-D)}{8L\left(\Delta V_0 / V_0\right) f^2} = 10.85 \text{ µF}$$

The design parameters of bi-directional converter used in proposed charging system are listed in Table 3.2.

Parameter	**Value**
Input DC voltage (V_s)	48V
Output DC voltage (V_0)	24V
Switching frequency (f)	10KHz
Bus capacitor (C_{Bus})	1000 µF
Parasitic bus resistance (R_{Bus})	0.1 m Ω
Filter inductance (L)	5.76 mH
ESR of inductor (R_L)	0.05 Ω
Filter capacitance (C)	10.85 µF
ESR of capacitor (R_C)	0.005 Ω
Load resistance (R_{Load})	180 Ω
Output voltage ripple (ΔV_0)	1%
Battery nominal voltage	24V
Battery rated capacity	50Ah
Initial SOC of battery	54%

Table 3.2: Design Specifications of Bi-Directional Converter

Closed-loop control is necessary to guarantee smooth and effective charging along with the appropriate charging current and voltage. In this work, the bi-directional converter is controlled in both the voltage and current modes using a proportional-integral (PI) controller. The battery voltage V_{Batt} and current I_{Batt} are precisely managed by the closed-loop control system, which keeps them at their respective reference levels, V_{Batt*} and I_{B_Ref}.

The real battery voltage V_{Batt} and current I_{Batt} are continuously compared to the reference values in order to operate the control mechanism. The PI controller receives the inconsistencies, or mistakes, that arise from these comparisons. After processing these mistakes, the PI controller produces the pulse-width modulation (PWM) signals required to operate the converter's two switches, S_1 and S_2.

In order to make certain that the battery charges at the required voltage and current levels during the charging phase, the PI controller alters the duty ratio of the PWM signals. In the same manner, the reference voltage is set to V_{Load*} during the discharging phase, and the PI controller employs the same method to control the discharging process, guaranteeing a steady and controlled transfer of energy to the load.

MATLAB/Simulink simulations, which offer a thorough examination of the closed-loop system's performance in both voltage and current modes, are used to assess the efficacy of this control technique. The control algorithm block diagram, shown in Fig. 3.8, shows how the PI controller works with the rest of the system to effectively handle the charging and discharging procedures.

The bi-directional battery charger circuit may precisely regulate the charging and discharging processes by employing a PI controller in this way, which improves the battery system's overall performance, dependability, and lifespan.

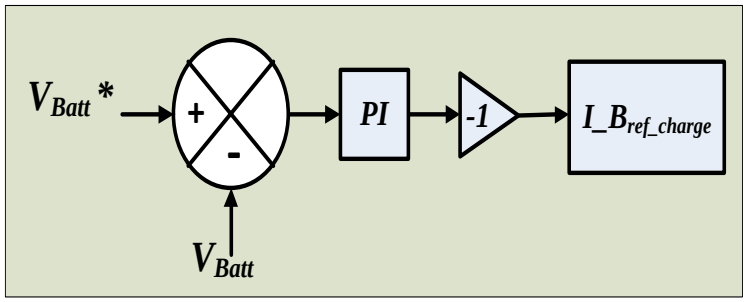

(a)

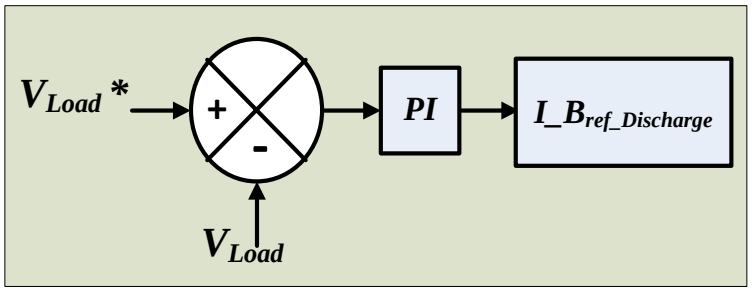

(b)

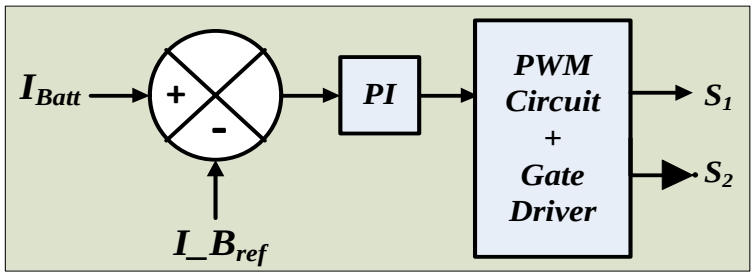

(c)

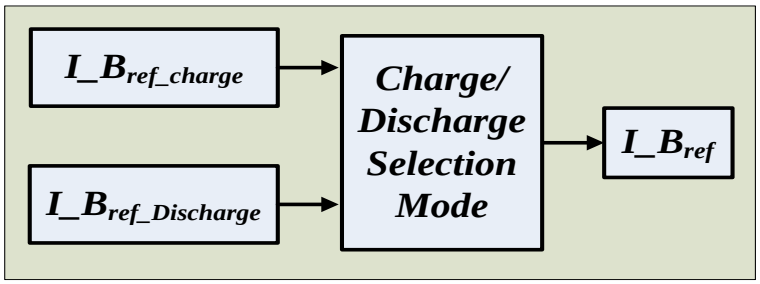

(d)

Fig. 3.8 Control algorithm of battery charging circuit (a) Battery voltage control (b) Load voltage control (c) Battery current control (d) Charge/Discharge selection mode

3.6 SIMULATION RESULTS

The efficiency of the provided ZCS switched-capacitor cell equalization circuit is demonstrated by the simulation results. Fig. 3.9 displays the initial cell voltages, which were [2.684V, 2.764V, 2.646V, 2.795V, 2.736V], highlighting the initial imbalance. After approximately 1.6 seconds of balancing, all cell voltages were equalized at 2.725V, which is the average of the initial voltages. This demonstrates the circuit's capability to efficiently balance the cells within a short period.

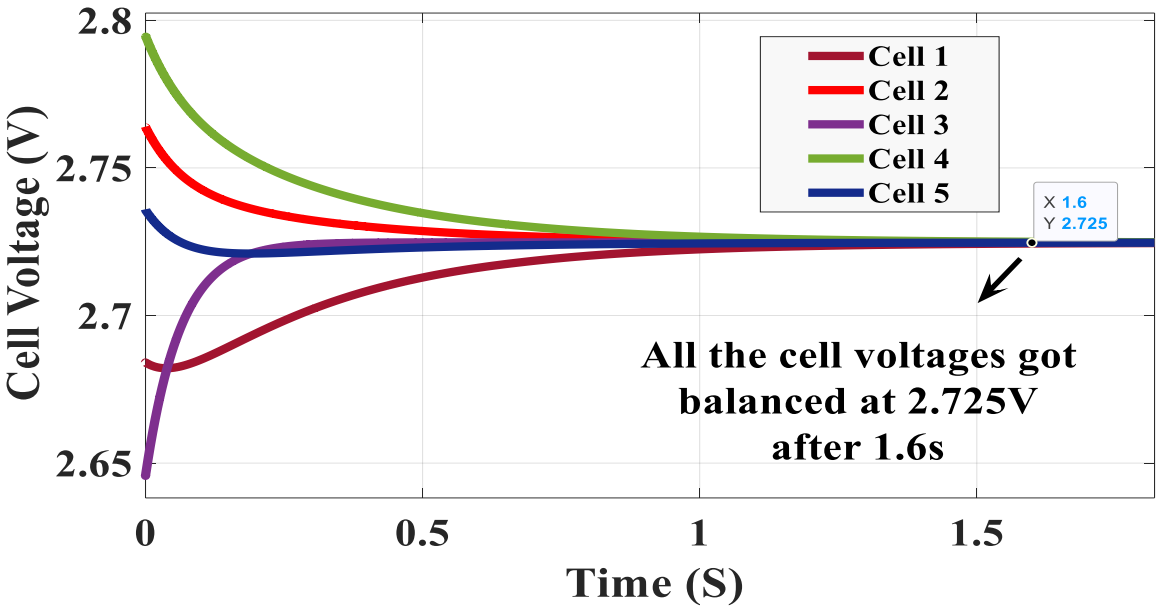

Fig. 3.9 ZCS Switched Capacitor Cell equalization results

Fig. 3.10 presents the capacitor current in the resonant tank and the current flowing through both switches. The capacitor current waveform follows a sinusoidal pattern, starting from zero, peaking, and then returning to zero at the end of each half-switch cycle. This sinusoidal behavior is crucial as it minimizes switching losses by ensuring that switches operate under zero-current conditions.

The voltage difference among the cells also shortens as the balancing process goes on, showing that the cells are becoming more balanced. As the cells get closer to equilibrium, the voltage and current in the capacitor correspondingly steadily drop, representing the decreased energy transfer needed. These outcomes verify the

circuit's design by demonstrating that it efficiently balances the cells and performs in a way that reduces energy losses and increases efficiency.

The simulation shows how quickly and efficiently the ZCS switched-capacitor cell balancing circuit can balance cell voltages, minimizing voltage differences between cells and reaching equilibrium in a short amount of time. This demonstration shows how the circuit can maintain steady cell voltages with little energy loss, increasing battery performance and life.

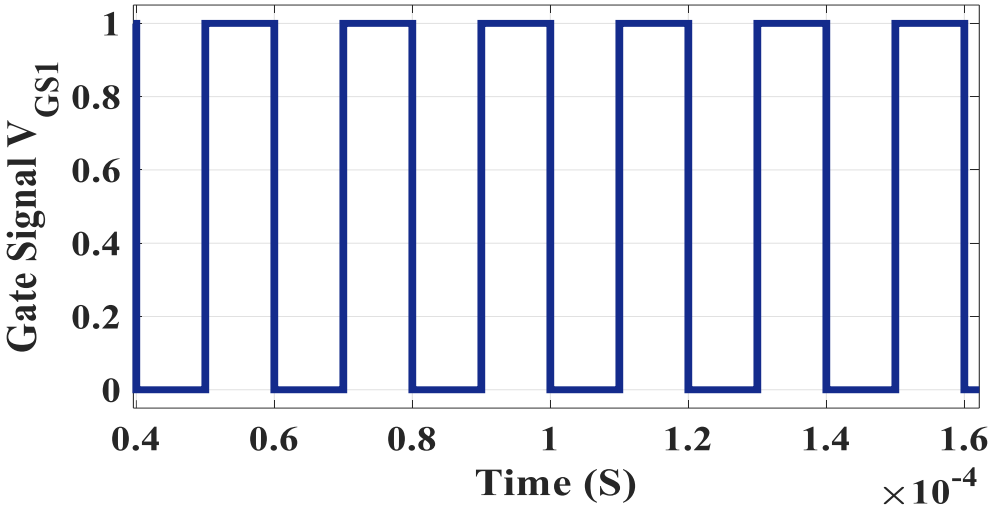

(a)

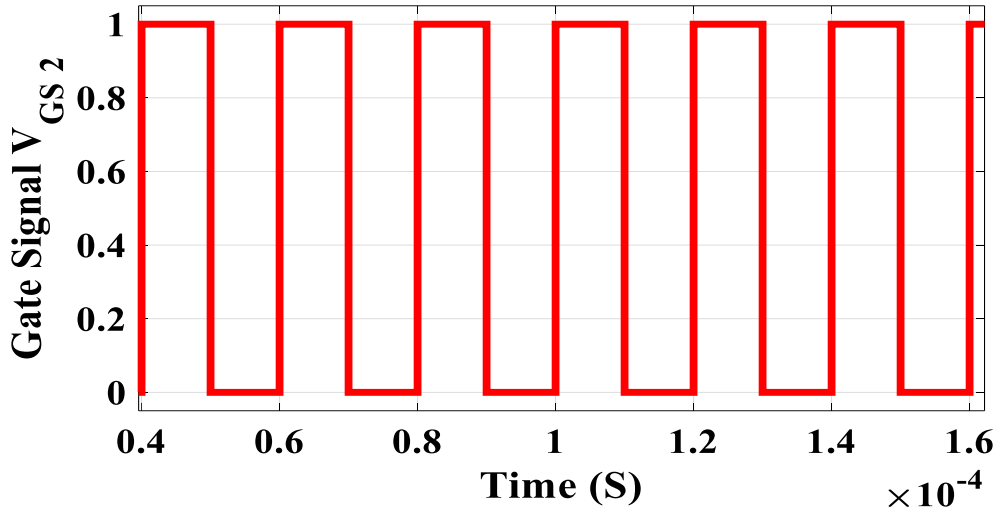

(b)

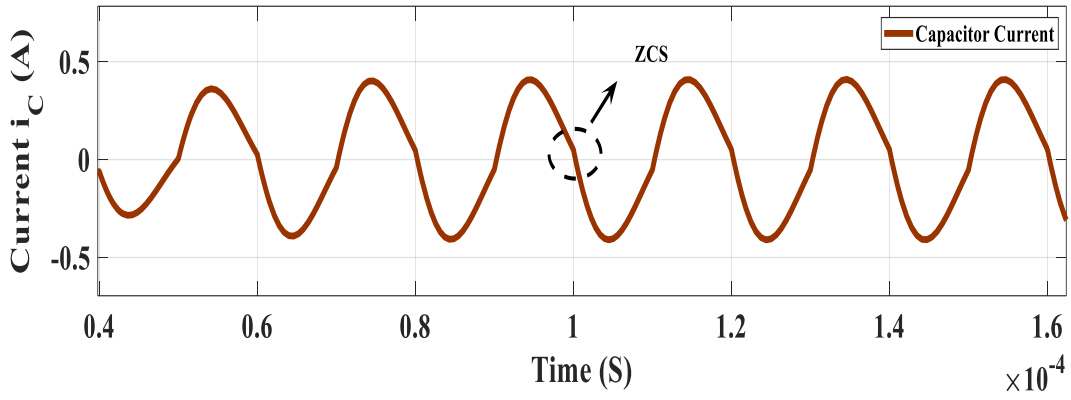

(c)

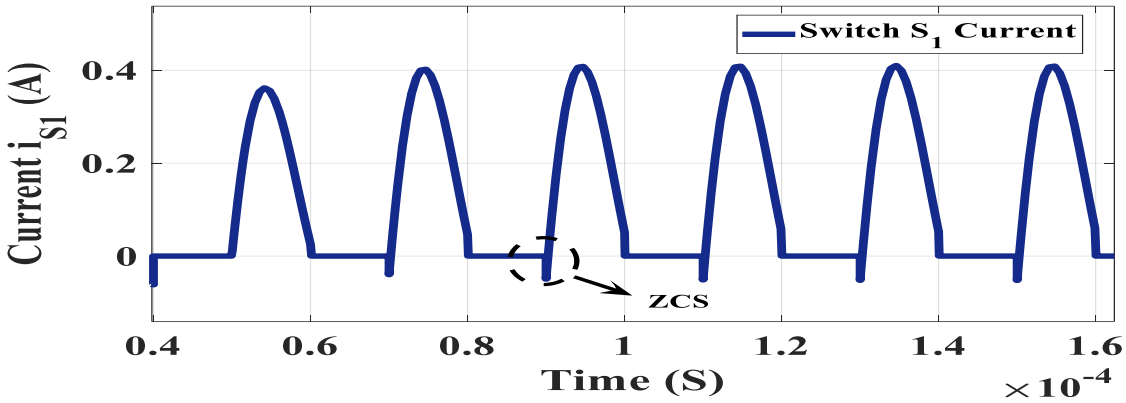

(d)

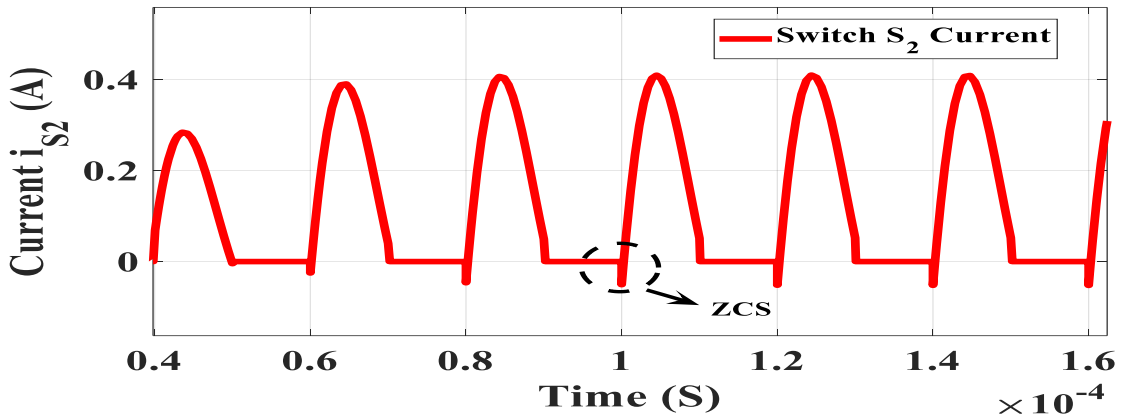

(e)

Fig. 3.10 Waveforms of gate signal to (a) Switch S_1. (b) Switch S_2. (c) Capacitor current. (d) Current through switch S_1 (e) Current through switch S_2

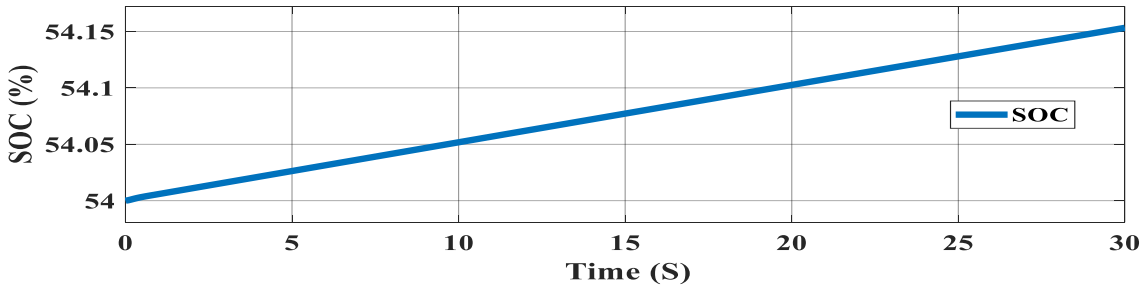

(a)

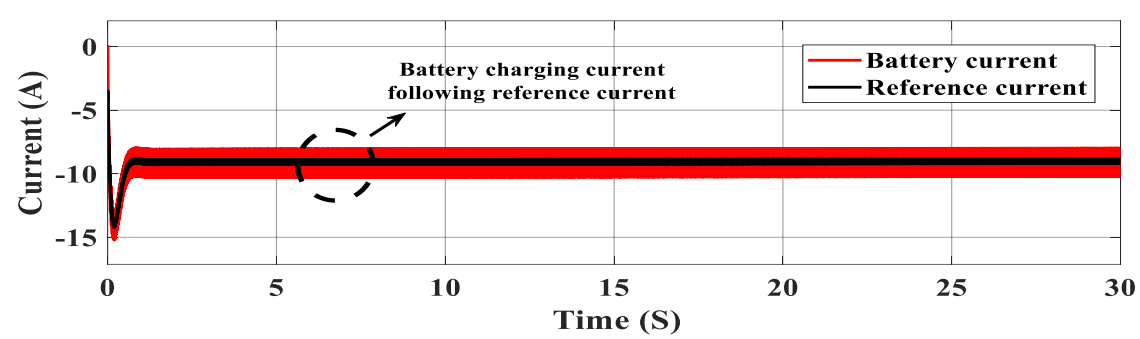

(b)

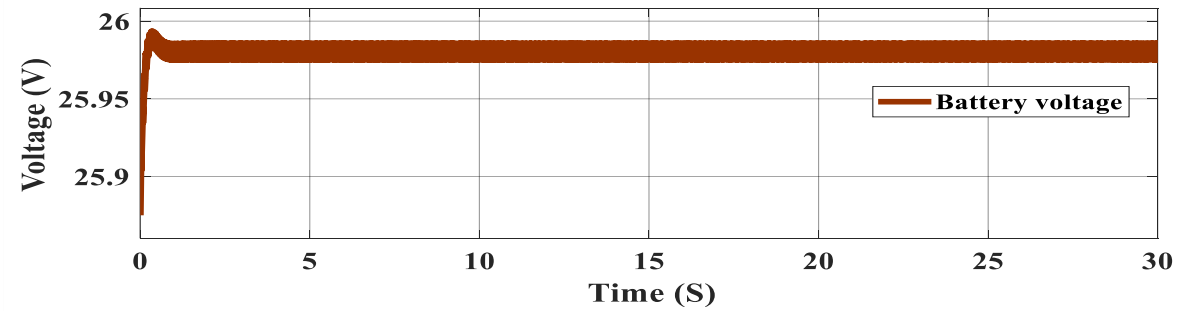

(c)

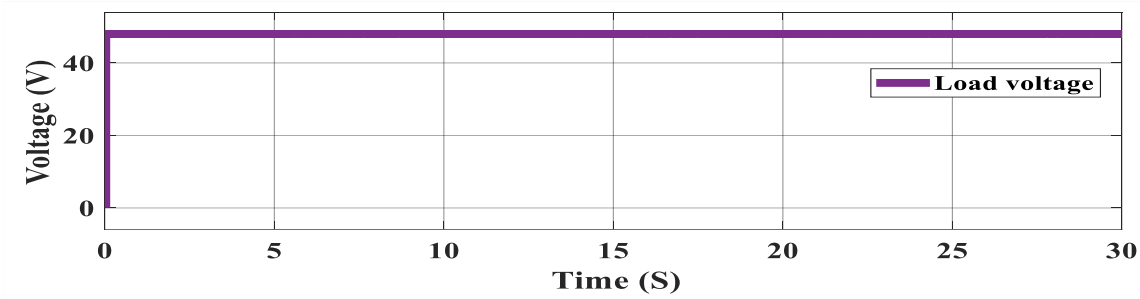

(d)

Fig. 3.11 Battery charging waveforms (a) SOC of battery while charging (b) Charging current (c) Battery voltage (d) Load voltage

Fig. 3.11, which displays the waveforms of the battery State of Charge (SOC), charging current (I_{Batt}), battery voltage (V_{Batt}), and load voltage (V_{Load}), illustrates the simulation results for the battery charging circuit. These waveforms show that the battery current waveform closely resembles the reference current, indicating the effectiveness of the control mechanism that was used. The maximum battery current in this case is 22A.

As the charging process advances, the charging current rapidly drops from its high starting point. In Constant Current (CC) mode, the battery current is made to be constant as the battery voltage steadily rises. Up until the battery reaches about 80% SOC, this mode is functional. The Constant Voltage (CV) mode of charging takes over when the battery voltage hits 25.98V. When in CV mode, the current starts to drop but the voltage stays constant. The source voltage (V_S) constantly supplies the load voltage (V_{Load}), which stays at 48V during the charging operation. The bi-directional battery charger circuit's reliability and efficacy in preserving the intended operating conditions are demonstrated by the steady load voltage. Fig. 3.12, which displays the waveforms of the battery State of Charge (SOC), charging current (I_{Batt}), battery voltage (V_{Batt}), and load voltage (V_{Load}), demonstrates the simulation results for both battery charging and discharging.

The current is shown as negative during the charging phase, indicating that current is entering the battery. The current changes to a positive value as the battery starts to deplete, indicating that current is now leaving the battery. When the battery is being discharged, the positive current indicates how much energy is being taken out to power the load.

Furthermore, the load voltage doesn't fluctuate from 48V during the charging or discharging process. This stability means that regardless of whether the battery is charging or draining, the load gets a steady and uninterrupted supply of power. The efficacy and dependability of the bi-directional battery charger are demonstrated by the circuit's capacity to maintain a constant load voltage during both phases. For applications that need a steady and dependable power source, it makes sure the connected load gets a continuous power supply.

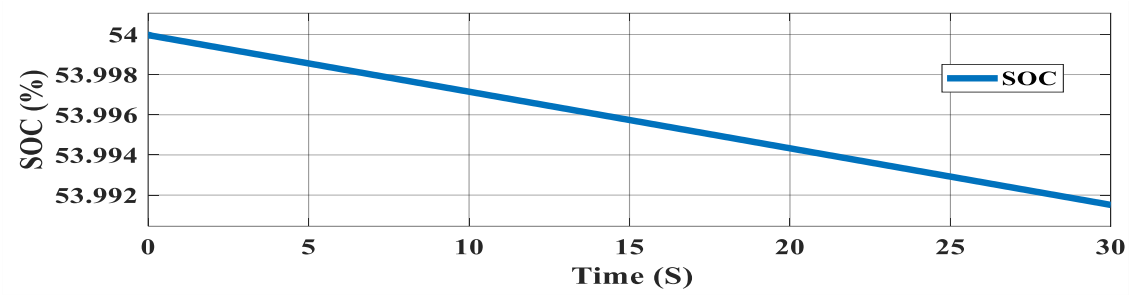

(a)

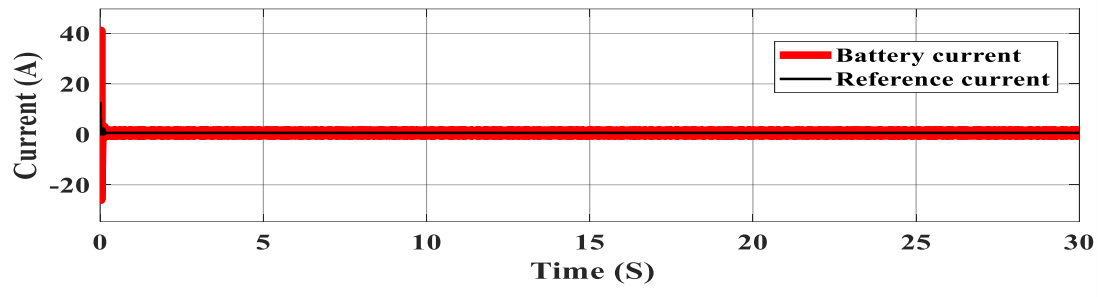

(b)

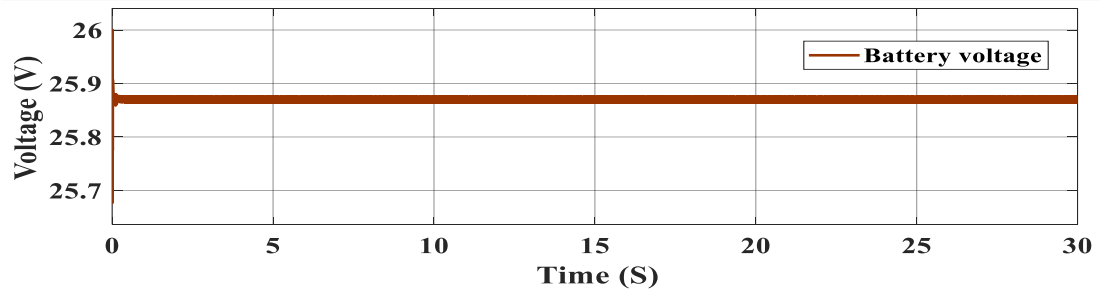

(c)

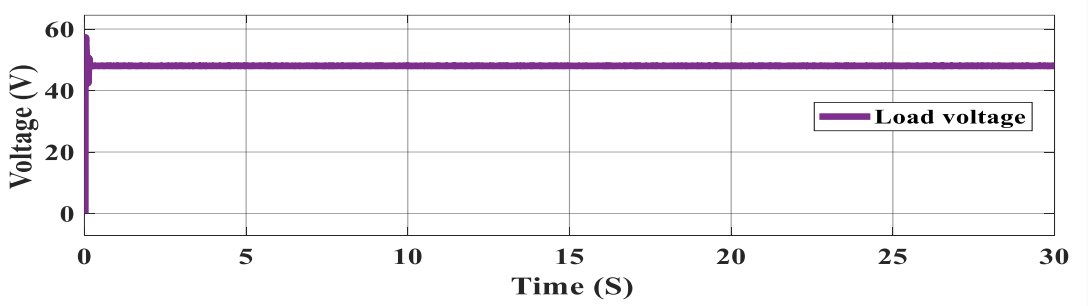

(d)

Fig. 3.12 Battery discharging waveforms (a) SOC of battery while discharging (b) discharging current (c) Battery voltage (d) Load voltage

3.7 CHAPTER SUMMARY

A bidirectional battery charging circuit integrated with a ZCS switching capacitor cell equalization scheme is presented in this chapter. The SC-based techniques described in this paper provide a number of benefits, one of which is the elimination of magnetic components, which reduces size and weight. On the other hand, when there are large voltage differences between cells, conventional SC-based cell balancing techniques frequently have reduced balancing efficiency, and the speed of balancing typically decreases as the gap between voltage level increases. A prominent drawback of traditional SC-based systems is that as the number of battery cells rises, their balancing speed decreases.

This problem is resolved by the suggested ZCS switching capacitor topology, which greatly increases the speed of balancing. According to the study, balancing the same number of cells with the same voltage imbalances can be completed in up to 1.6 seconds less time than with traditional SC topologies. Faster balancing not only increases performance but also lowers system losses in batteries with many series-connected cells, therefore this enhancement is especially advantageous for those batteries.

Additionally, by combining the balancing circuit with a bidirectional battery charging circuit, the study expands the utility of the circuit. Through this integration, a DC-DC converter can be used to charge or discharge the battery pack in either way. When the battery has to be charged, the converter steps down the input voltage in buck mode. When the battery needs to be discharged, it steps up the battery voltage in boost mode to maintain a constant voltage across the load. This bidirectional converter is skilfully managed by the closed-loop PI controller, guaranteeing peak performance in both charging and discharging modes.

Through extensive verification with MATLAB/Simulink simulations, the outcomes and discussions presented in this work show the effectiveness and dependability of the suggested ZCS switched capacitor cell balancing topology with buck-boost capability.

CHAPTER 4
BUCK-BOOST + CUK CONVERTER CELL BALANCING CIRCUIT

4.1 INTRODUCTION

Both the buck-boost and Cuk converters are widely employed in battery equalization applications because of their modular versatility and capacity to produce negative output voltages. The buck-boost converter is well-known for being easy to use and having the capacity to adjust voltage, which makes it appropriate for a range of battery balancing applications. But it needs a lot of switches and inductors, which can make the design more difficult and expensive. The steady input and output currents provided by the Cuk converter, on the other hand, lessen the strain on the battery cells and increase overall efficiency. As in the case of the buck-boost converter, the Cuk converter also requires a large number of components in spite of these advantages. Traditional buck-boost and Cuk converters have a lot of switch requirements, which is their main drawback. For example, $2n-1$ switches are usually required to equalize a string of n battery cells, which increases complexity and may cause reliability problems. Moreover, the control and management of these converters become increasingly difficult as the number of cells connected in series increases. This frequently leads to higher device voltage stress and complex control procedures.

This chapter describes a bidirectional DC-DC converter for series-connected battery cell balancing that blends cuk and buck-boost converters. Conventional techniques for balancing n battery cells usually call for two $n-1$ switches that use cuk converters or buck-boost converters. The suggested buck-boost + Cuk converter, on the other hand, practically halve the number of switches needed without sacrificing the benefits of modularization or raising device voltage stress by combining these two converters. One important aspect of buck-boost equalizers is that this design preserves the simplicity of pulse width modulation (PWM) at a 50% duty cycle.

Its modular design increases flexibility by making it easy to add or remove cells from the string.

This chapter also incorporates a battery charging circuit based on a SEPIC converter, as addition to the buck-boost + Cuk converter. This integration enables effective and flexible battery management, much to the method used in Chapter 3 with the buck-boost converter bi-directional battery charger circuit. With consistent voltage across the load and best-in-class battery performance, the SEPIC converter offers a reliable option for charging and discharging processes. This integrated system provides a complete solution for high voltage battery packs while improving the battery management system's overall functionality and efficiency.

4.2 SYSTEM CONFIGURATION

With fewer switches and parts, the system is made to effectively balance a number of battery cells in this combination buck-boost + Cuk converter topology (Fig. 4.1). Figure 4.2 shows an example of a four-cell battery. This innovative topology, in contrary to the conventional buck-boost converter, removes the requirement for buck-boost converters on the left side of the battery string, which results in the removal of two switches and one inductor. Rather, a single capacitor is added to the right side to facilitate energy transmission between the cells at the top and bottom, therefore converting the central converter into a Cuk converter. The normal buck-boost converter has limitations when it comes to transferring energy between nearby cells; this design, on the other hand, allows for energy transfer over the entire battery string.

Because of the high degree of modularity in the suggested system layout, adding or removing cells from the battery string is simple. Applications that need to be flexible and scalable, including large-scale energy storage systems and electric vehicles, can benefit greatly from this flexibility. Thus, a reliable, effective, and scalable solution for battery cell balancing is offered by the combined buck-boost + Cuk converter, guaranteeing the best possible performance and longevity of high voltage battery packs.

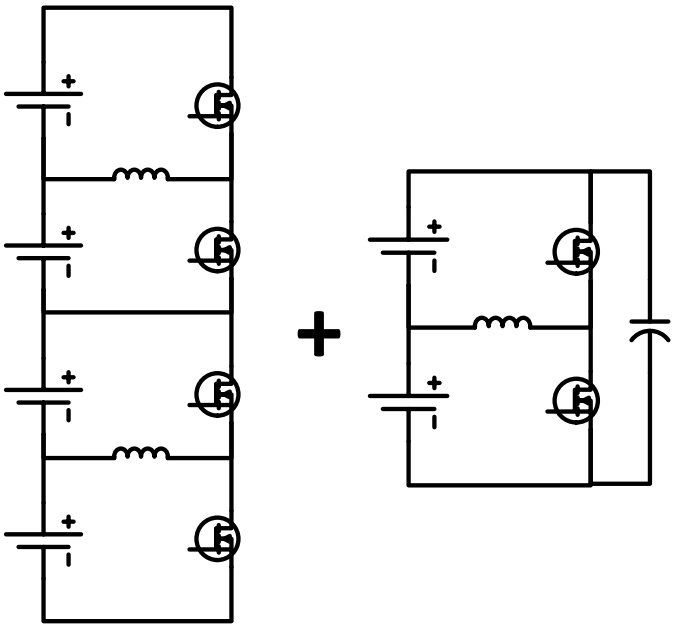

(a) (b)

Fig. 4.1 Combining circuits of (a) Buck-Boost converter (b) Cuk converter

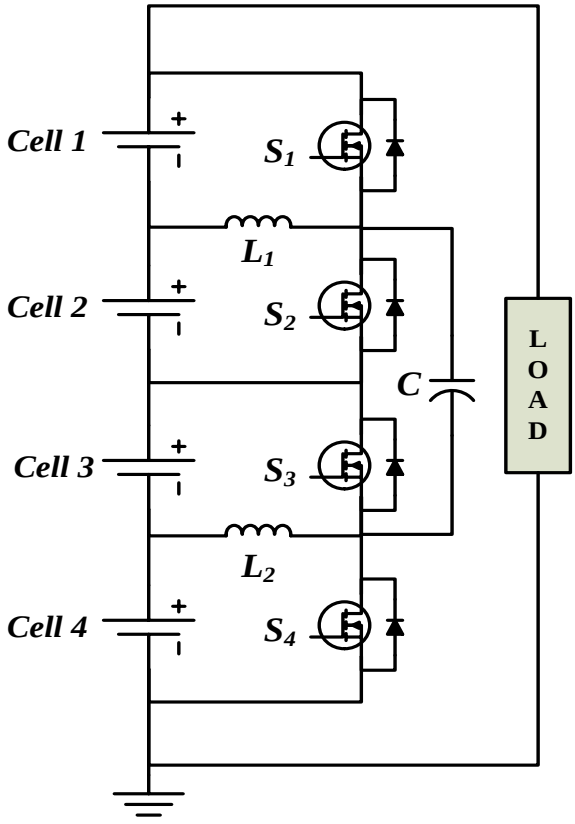

Fig. 4.2 System configuration of the buck-boost + cuk converter for 4 cells

4.3 MATHEMATICAL ANALYSIS

This section presents a thorough mathematical study of the circuit that balances the buck-boost + Cuk converter cell. This converter's design makes it scalable and efficient by balancing battery cells with a small number of components. In particular, n switches (one for each cell), $n/2$ inductors, and $(n-2)/2$ capacitors are needed for the equalizer. The voltage of the battery pack has no bearing on this design, which can scale to any number of battery cells. The analysis will concentrate on a string of four batteries for simplicity's sake.

The following control approach is used to balance the battery cells in this topology:

- Cells 1 and 2 are equalized using the conventional buck-boost converter by applying a 50% duty cycle to switches S_1 and S_2.
- In a similar vein, cells 2 and 3 are equalized using the Cuk converter in the center by manipulating switches S_2 and S_3 with a 50% duty cycle. Cells 3 and 4 are equalized by using the lower buck-boost converter similarly.

With S_1 being complementary to S_2, S_2 being complementary to S_3, and S_3 being complementary to S_4, this method guarantees that each switch runs at 50% duty cycle. With dead time ignored and assuming that $V_1 > V_2$ and $V_3 > V_4$, we can explain how the circuit operates in two switching states, as shown in Fig. 4.3.

Switches S_1 and S_3 are activated while S_2 and S_4 are disabled in State I, as shown in Fig. 4.3(a). The voltage of battery cell 1, V_1, is equal to the voltage across the top inductor L_1. Through switch S_1, battery cell 1 releases its energy into inductor L_1, increasing the current through it linearly.

Similarly, the voltage across battery cell 3 (V_3) is equal to the voltage across the bottom inductor L_2. Here, switch S_3 allows inductor L_2 to receive a charge from cell 3 energy. $V_1 + V_2$ will be the voltage across the energy transfer capacitor C. Battery cell 4 is left inactive at this time since S_4 is switched off, but battery cell 2 is being charged by the energy transfer capacitor C through L_1 and S_3.

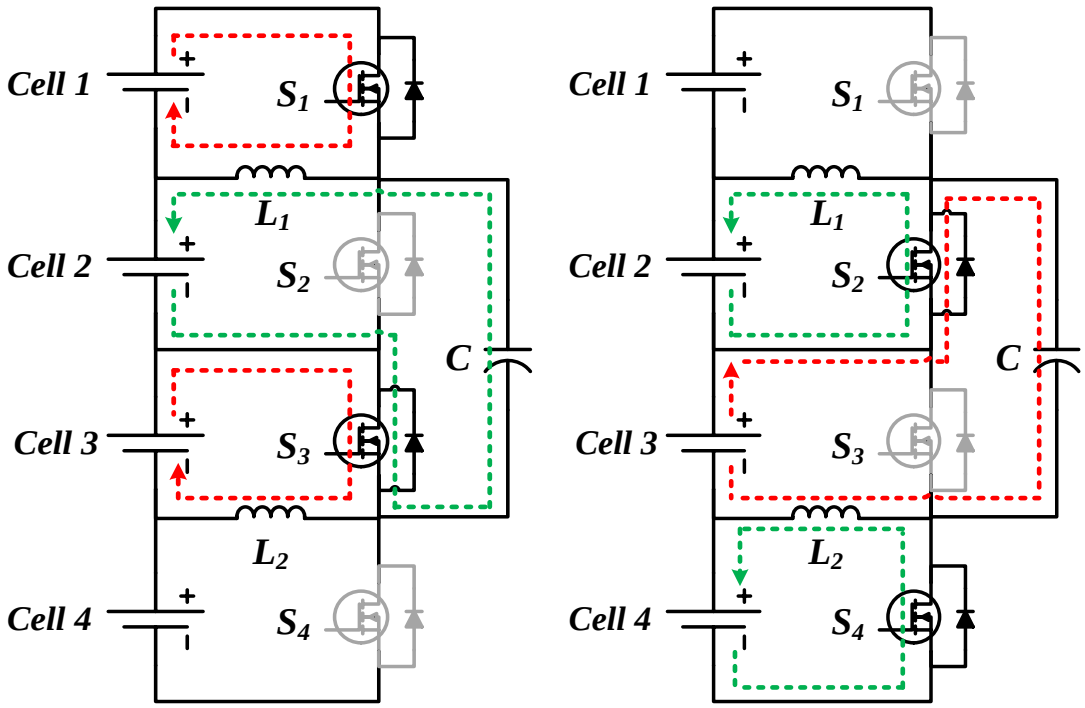

(a) (b)

Fig. 4.3 Modes of operation (a) State I (b) State II

The voltage across the inductor L_1, in charging phase is given by,

$$V_{L1} = V_{cell\,1} = L\frac{d_{iL1}}{dt} \tag{4.1}$$

By applying KVL we get,

$$V_{cell\,2} = V_C - V_{L1} \tag{4.2}$$

The voltage across the inductor L_2, in charging phase is given by,

$$V_{L2} = V_{cell\,3} = L\frac{d_{iL2}}{dt} \tag{4.3}$$

For the expression of capacitor current we apply KCL,

$$i_{L1} = i_{cell\,1} + i_C \tag{4.4}$$

Here in this case, cell 1 current is same as current through the switch S_1

Switches S_2 and S_4 are activated in State II, whereas S_1 and S_3 are disabled, as shown in Fig. 4.3(b). The voltage of battery cell 2, V_2, is equal to the voltage across the top inductor L_1. Battery cell 2 charges through the energy of the inductor L_1 via switch S_2, maintaining the same current direction, which causes the current through L_1 to drop linearly.

Similarly, the voltage across battery cell 4 (V_4) is equal to the voltage across the inductor L_2 at the bottom. Here, switch S_4 allows inductor L_2 to release its energy into cell 4. V_3 + V_4 will be the voltage across the energy transfer capacitor C. While battery cell 1 is dormant and does nothing because S_1 is turned off, battery cell 3 charges the capacitor C through L_2 and switches S_2, storing energy in the capacitor during this time.

The voltage across the inductor L_1 in discharging phase is given by,

$$V_{L1} = -V_{cell\,2} = L\frac{d_{iL1}}{dt} \tag{4.5}$$

By applying KVL we get,

$$V_{cell\,3} = V_C + V_{L2} \tag{4.6}$$

The voltage across the inductor L_2, in discharging phase is given by,

$$V_{L2} = -V_{cell\,4} = L\frac{d_{iL2}}{dt} \tag{4.7}$$

For the expression of capacitor current we apply KCL,

$$i_{L2} = i_{cell\,4} + i_C \tag{4.8}$$

Here in this case, cell 4 current is same as current through the switch S_4.

During operation, the voltage differentials between the battery cells dictate which way current flows through inductors L_1 and L_2. Because of this inherent feature of the circuit, controlling the current flow doesn't require any outside intervention, which simplifies the control plan. Consequently, battery cells 1 and 3 are continuously draining, whereas cells 2 and 4 are continuously charging, supporting the original hypothesis that cells $V_1 > V_2$ and cells $V_3 > V_4$.

4.4 SEPIC CONVERTER BASED BATTERY CHARGER CIRCUIT

DC-based charging systems for electric vehicles and home distribution have grown more and more appealing with the advent of renewable energy sources. Buck-boost converters are more affordable since they just need a single inductor and a capacitor. Nonetheless, there is a noticeable amount of input current ripple with these converters. Harmonics, which can be produced by this ripple, frequently necessitate the use of an LC filter or a sizable capacitor. As a result, the buck-boost is frequently costly or ineffective. Another issue that can make employing buck-boost converters more challenging is their tendency to reverse voltage. SEPIC converters solve these problems. The Single-Ended Primary-Inductor Converter (SEPIC) is one type of DC-DC converter that can produce an output voltage that is greater than, less than, or equal to its input voltage. The SEPIC converter combines the ideas of an inverted buck-boost converter and a boost converter to provide a non-inverted output. A DC voltage source V_S, an inductor L_1 connected in series with the input voltage source, a switch SW, and a complementary diode D make up the SEPIC converter, as shown in Fig. 4.4. The energy flow is regulated by the diode, coupling capacitor C_1, and switch together. With the coupling capacitor and the diode, inductor L_2 forms a T-junction by hanging between the input and output sides. By connecting the battery pack—the item being charged or discharged—in parallel with the output capacitor, a constant voltage is guaranteed at the battery pack's input terminals.

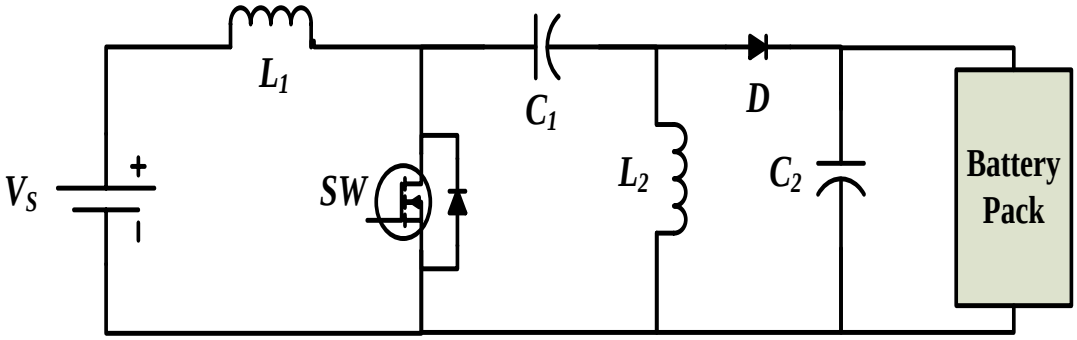

Fig. 4.4 SEPIC converter

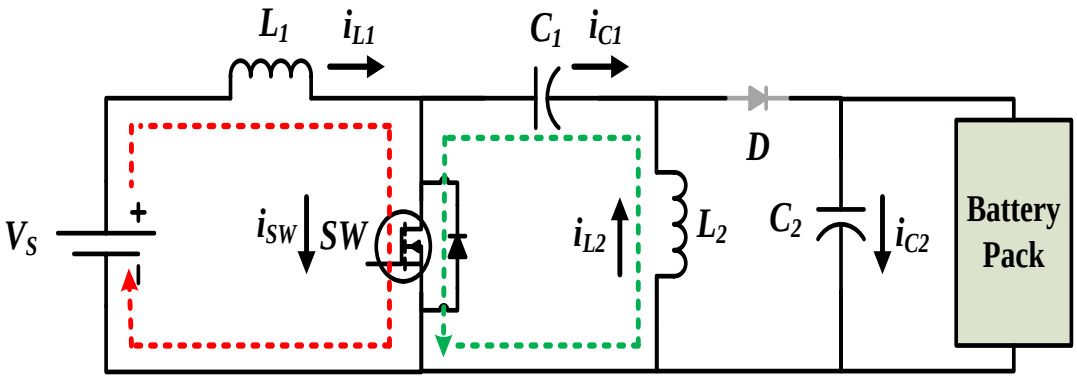

(a)

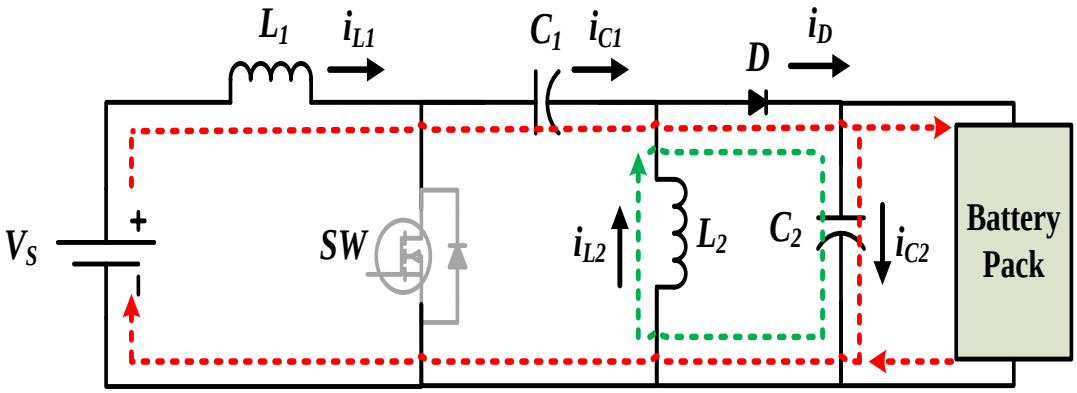

(b)

Fig. 4.5 SEPIC converter modes of operation (a) Mode I (b) Mode II

To ensure effective battery charging and system protection under varied input voltages, the SEPIC converter battery charger typically functions in two modes.

In **Mode I**, diode D is reverse biased and the switch SW is activated. The current through the inductor L_1 then increases linearly when the input voltage, V_S, is applied across it. In this mode, the coupling capacitor C_1 charges and releases its stored energy into the inductor L_2. By keeping the output voltage V_0 and current I_{Batt} constant, this procedure makes sure that the battery pack charges continuously. Fig. 4.5 (a) shows this mode, which is essential for preserving the battery's charge at higher voltage levels.

In **Mode II**, the diode D becomes forward biased and the switch SW is disabled. The battery pack serves as the load in this instance, receiving constant voltage from the inductors L_1 and L_2. Both inductors release the energy they have accumulated. In this mode, the discharge of inductor L_1 charges the coupling capacitor. The inductor transfers its stored energy to the output, simulating the actions of a boost converter. This guarantees that power to the battery pack is supplied continuously. This mode, which is shown in Fig. 4.5(b), is essential to keeping the battery pack's power supply steady.

The SEPIC converter efficiently handles various input situations by smoothly transitioning between these two modes, guaranteeing dependable battery charging and peak system performance.

4.5 DESIGN AND CONTROL

Each battery cell is modelled as a capacitor with an initial voltage and capacitance value for simplicity's sake. This topology exerts the same amount of demand on the switches as buck-boost and cuk converter balancing, or 2 V_{Cell_max}. Thus, this must be considered while selecting the switch with the proper rating, where V_{Cell_max} is the highest voltage of all the cells connected in series.

The cuk converter module is the function of the capacitor used in this cell balancing circuit. In mode I, the maximum voltage across it is equal to $V_1 + V_2$, and in mode II, it is equal to $V_3 + V_4$. Since we are unsure which voltage combination will result in more stress, we can conclude that 2 V_{Cell_max} will be the maximum stress across the capacitor. For the suggested balancing circuit, both kinds of ceramic and polyester film capacitors are advised in order to reduce the parasitic resistance.

The main differences of the two types of capacitors are that:

(i) Despite having the same voltage rating and capacitance, polyester film capacitors are larger than ceramic capacitors;

(ii) Polyester film capacitors have a relatively stable capacitance throughout a wide range of DC bias voltages, whereas ceramic capacitors see a decrease in capacitance as their DC bias voltage increases. Additionally, the equivalent series inductance (ESL) of ceramic capacitors is less.

Hence, when ceramic capacitor should be selected for the proposed balancing circuit.

For simplicity, all of the inductors used in the suggested cell equalizing circuit ought to have the same inductance L and be made with buck-boost/cuk converter design concerns in mind.

MOSFET on-state resistance (R_{ON}) should be as low as feasible to minimize losses and overall parasitic resistance R. On the other hand, there is an inverse correlation between the on-state resistance and the MOSFET's gate-to-source. This suggests that a lower R_{ON} causes a higher C_{GS}, which somewhat increases the gate driving losses. Consequently, an extremely low R_{ON} is not possible.

For the balancing process to go more quickly, a higher switching frequency is advised. greater gate driving loss, however, is associated with greater switching frequencies. In order to preserve overall efficiency, the gate driving losses are especially important for this balancing circuit.

Parameter	Value
Cell 1	2.764V
Cell 2	2.684V
Cell 3	2.795V
Cell 4	2.646V
Capacitance of each cell	0.5F
Switching frequency (f_s)	100KHz
MOSFET on state resistance (R_{ON})	0.96mΩ
Module capacitance (C)	100µF
Module inductance (L_1, L_2)	20µH

Table 4.1: Design Specifications of Buck-Boost + Cuk converter equalizing circuit

The purpose of the SEPIC converter is to offer a versatile and effective solution for battery charging applications. Despite changes in the input voltage, the SEPIC converter's architecture enables it to maintain a constant output voltage.

The input voltage to SEPIC converter is take to be 40V and by keeping the duty ratio in or around 34%, the output voltage (which is also the input voltage to the cell balancing circuitry) is maintained constant around 20V.

$$D = \frac{V_0}{V_0 + V_{in}} = 0.34$$

The output power is taken around 50W to maintain the charging current of around 2.5A

$$I_{out} = \frac{P_{out}}{V_0} = 2.5\ A$$

Average inductor current through L_1 is given by,

$$I_{L1(avg)} = \frac{V_0\ *\ I_0}{V_{in}} = 1.25\ A$$

$$I_{L2(avg)} = \ I_{out} = 2.5\ A$$

The inductor is made to work in continuous conduction mode (CCM) to simplify the analysis.

Assuming current ripple to be around 5%, inductor value is calculated as

$$L_1 = \frac{V_{in} * \mathrm{D}}{\Delta i_{L1}\, f} = 2.18\ \mathrm{mH}$$

$$L_2 = \frac{V_{in} * \mathrm{D}}{\Delta i_{L2}\, f} = 1.08\ \mathrm{mH}$$

Considering a voltage ripple of 1%, capacitor value is calculated as

$$C_1 = \frac{V_0 * \mathrm{D}}{\mathrm{R}\, \Delta v_C\, f} = 42.5\ \mu\mathrm{F}$$

$$C_2 = \frac{V_0 * \mathrm{D}}{\mathrm{R}\, \Delta v_C\, f} = 42.5\ \mu\mathrm{F}$$

Parameter	**Value**
Input DC voltage (V_{in})	40V
Output DC voltage (V_0)	20V
Duty cycle (D)	33.4 %
Switching frequency (f)	100KHz
Inductor (L_1)	2.176 mH
Inductor (L_2)	1.088 mH
Coupling capacitor (C_1)	42.5 µF
Output capacitor (C_2)	42.5 µF
Load resistance (R)	8 Ω
Output voltage ripple (Δv_c)	1%
Current ripple ($\Delta i_{L1}, \Delta i_{L2}$)	5%

Table 4.2: Design Specifications of SEPIC converter charging circuit

4.6 SIMULATION RESULTS

The simulation results show how well the Buck-Boost + Cuk converter cell balancing circuit balances. The initial cell voltages are displayed as [2.764V, 2.684V, 2.795V, 2.646V] in Fig. 5.6, which clearly reveals an imbalance. The circuit effectively equalized all cell voltages to 2.72V, the average of the initial values, after operating for around 0.4 seconds. This demonstrates that the circuit can quickly and efficiently balance the cells.

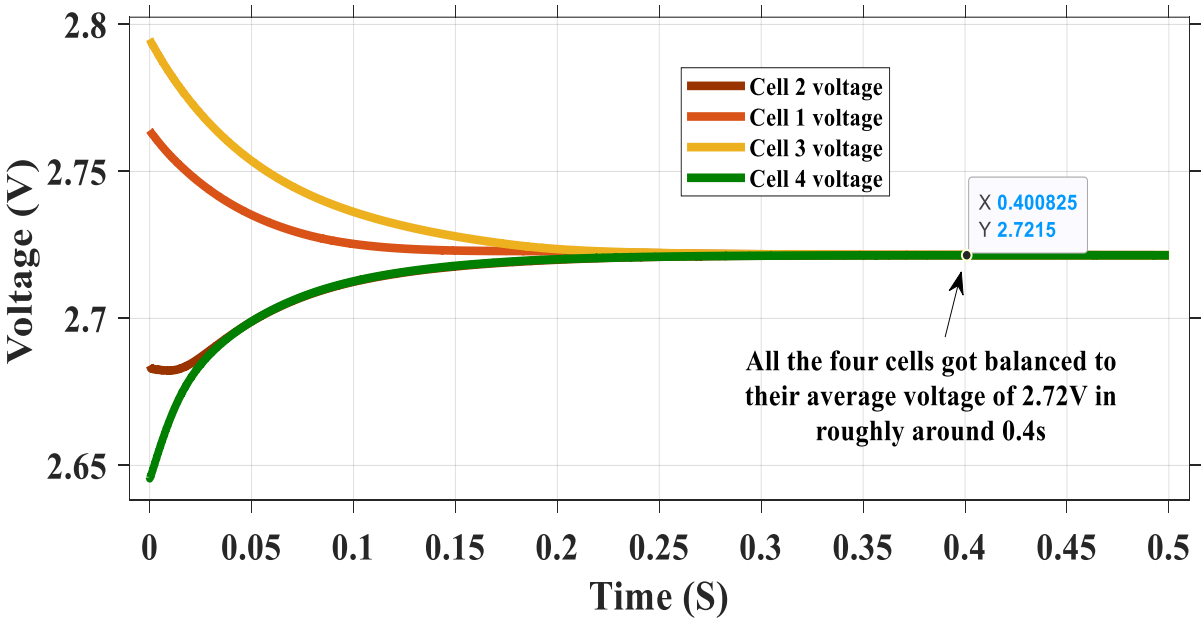

Fig. 4.6 Buck-Boost + Cuk converter Cell equalizing results

The voltage difference between the cells lessens as the balancing process goes on, showing that the cells are becoming more balanced. As the cells get closer to equilibrium, the voltage and current in the capacitor correspondingly steadily drop, representing the decreased energy transfer needed. These outcomes verify the circuit's design by demonstrating how well it balances the cells.

The simulation results of cell balancing with a battery charger based on a SEPIC converter are shown below.

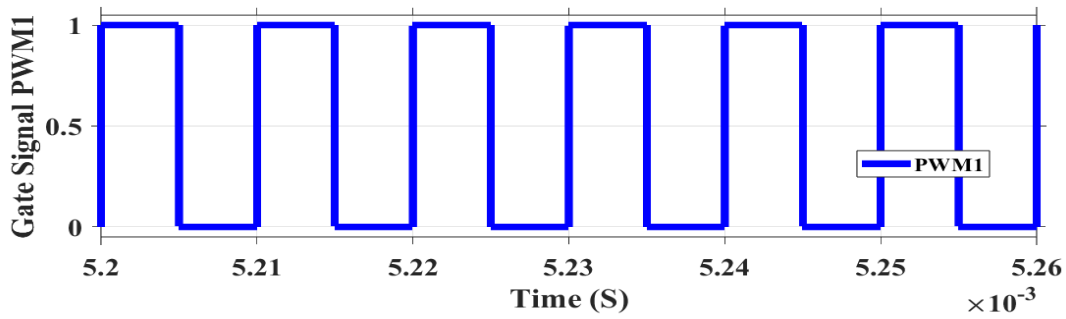
Gate Signal PWM1
1
0.5
0
PWM1
5.2
5.21
5.22
5.23
5.24
5.25
5.26
Time (S)
×10-3

(a)

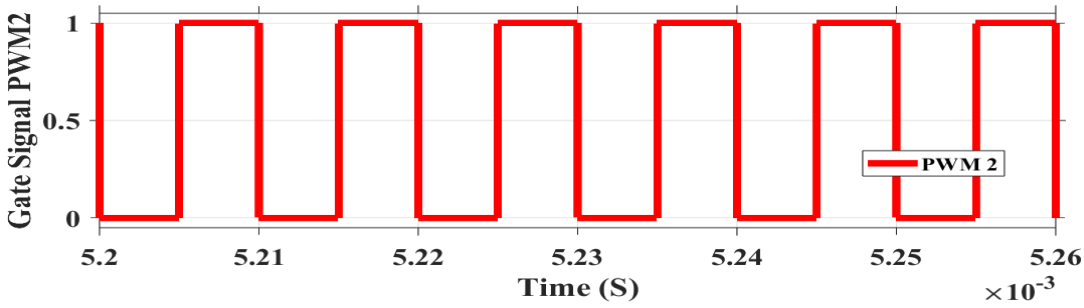
Gate Signal PWM2
1
0.5
0
PWM 2
5.2
5.21
5.22
5.23
5.24
5.25
5.26
Time (S)
×10-3

(b)

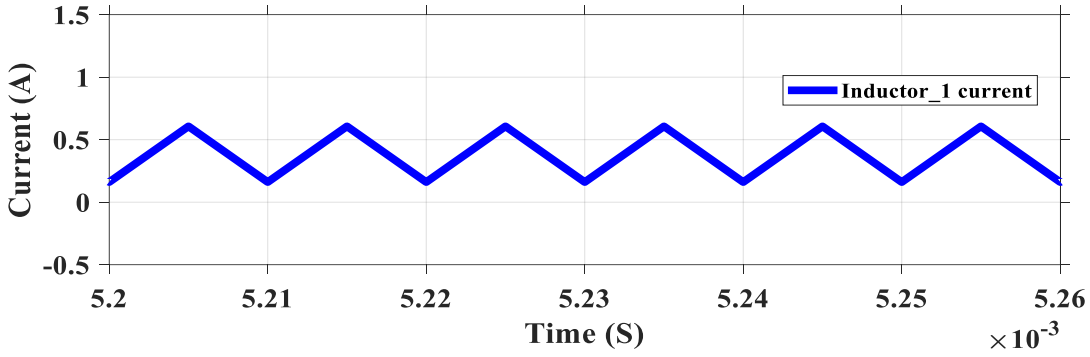
Current (A)
1.5
1
0.5
0
-0.5
Inductor_1 current
5.2
5.21
5.22
5.23
5.24
5.25
5.26
Time (S)
×10-3

(c)

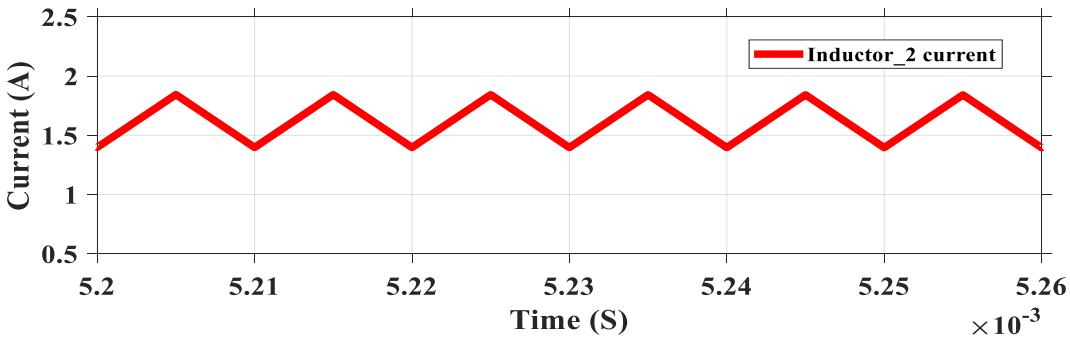
Current (A)
2.5
2
1.5
1
0.5
Inductor_2 current
5.2
5.21
5.22
5.23
5.24
5.25
5.26
Time (S)
×10-3

(d)

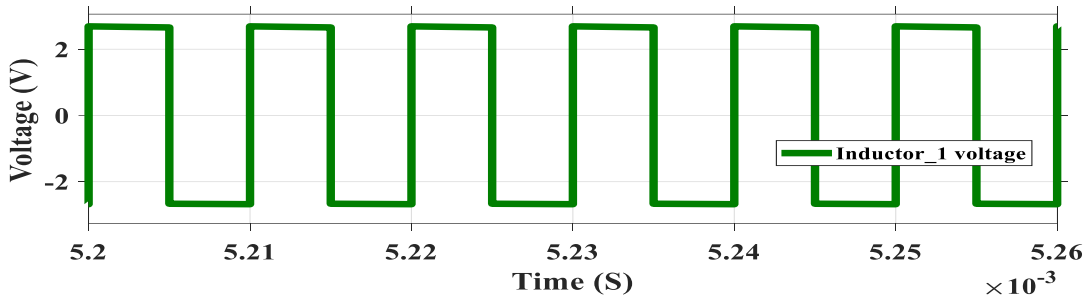
Voltage (V)
2
0
-2
Inductor_1 voltage
5.2
5.21
5.22
5.23
5.24
5.25
5.26
Time (S)
×10^-3

(e)

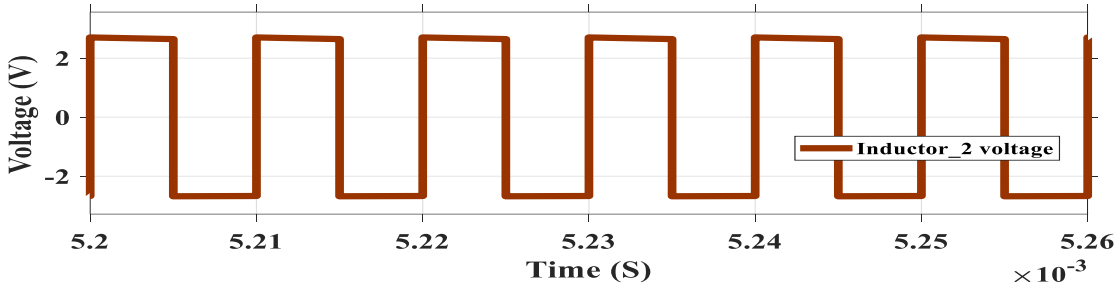
Voltage (V)
2
0
-2
Inductor_2 voltage
5.2
5.21
5.22
5.23
5.24
5.25
5.26
Time (S)
×10^-3

(f)

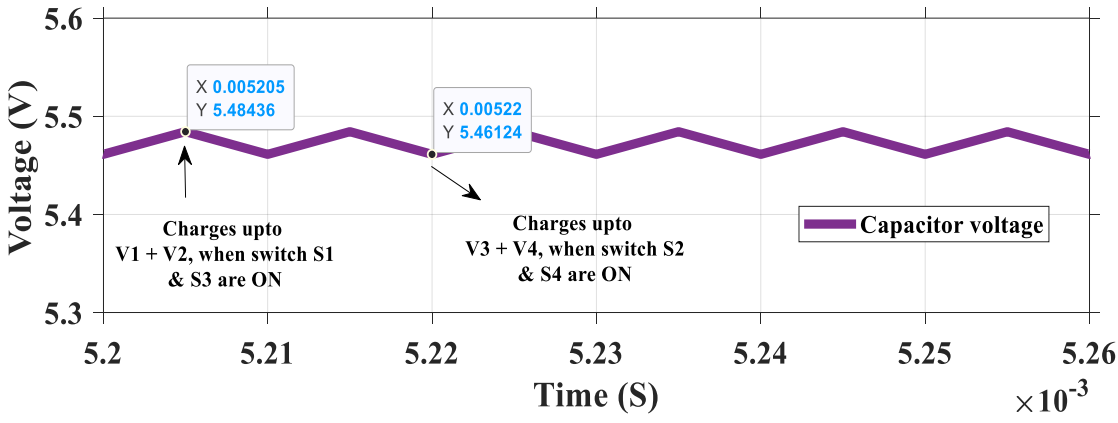
Voltage (V)
5.6
5.5
5.4
5.3
X 0.005205
Y 5.48436
X 0.00522
Y 5.46124
Charges upto
V1 + V2, when switch S1
& S3 are ON
Charges upto
V3 + V4, when switch S2
& S4 are ON
Capacitor voltage
5.2
5.21
5.22
5.23
5.24
5.25
5.26
Time (S)
×10^-3

(g)

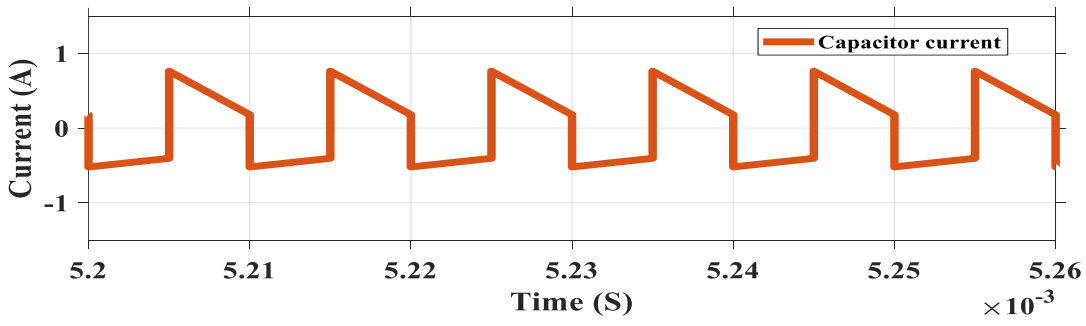
Current (A)
1
0
-1
Capacitor current
5.2
5.21
5.22
5.23
5.24
5.25
5.26
Time (S)
×10^-3

(h)

Fig. 4.7 (a) and (b) presents the gate signals given to four switches in the circuit. PWM1 signal is given to the switches S_1 and S_3, while signal PWM2 is given to the switches S_2 and S_4 respectively, (c) and (d) depicts the inductor current waveforms in the circuit, indicating charging and discharging for 50% of time period, (e) and (f) illustrates both the inductor voltages, and the volt-sec balance, (g) and (h) shows the capacitor voltage and capacitor current waveforms.

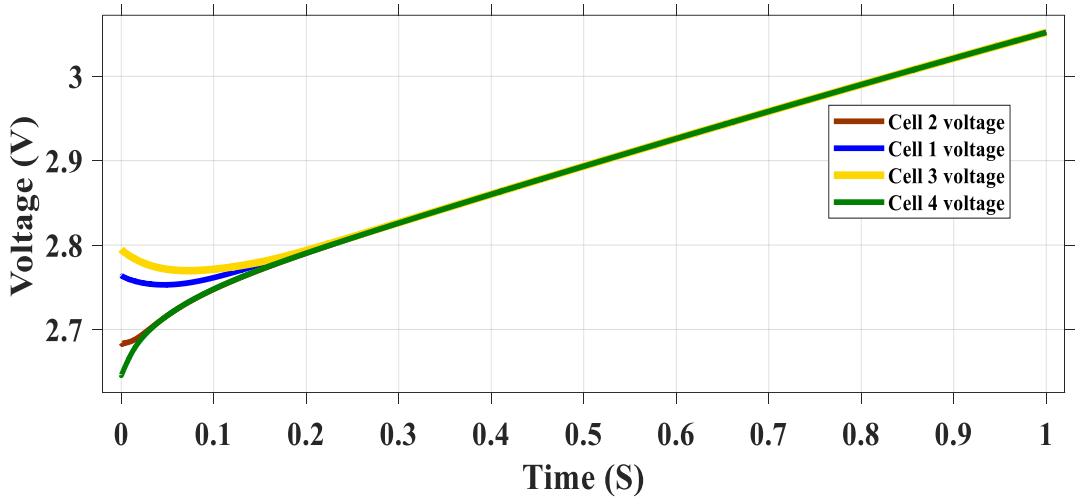

(a)

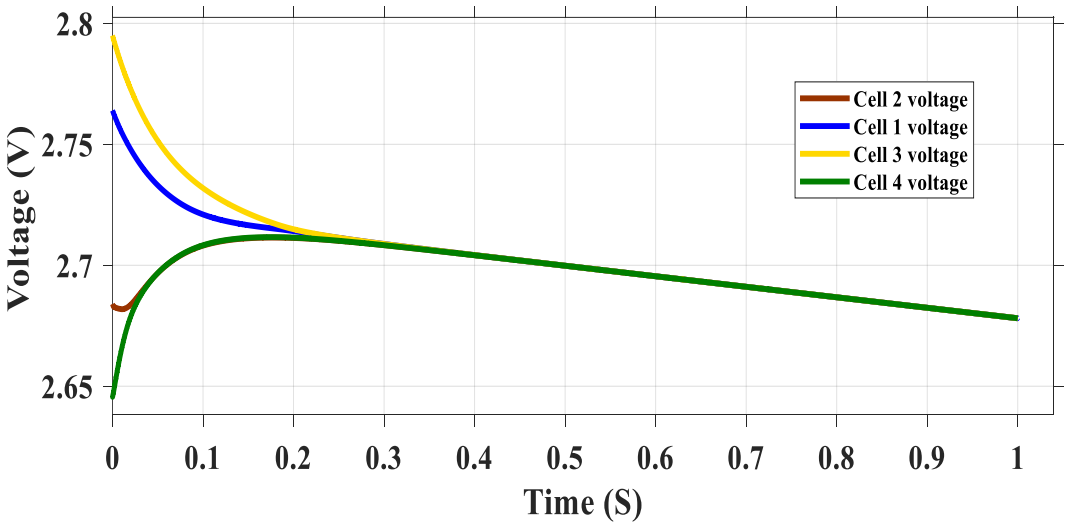

(b)

Fig. 4.8 (a) represents the battery pack charging along with the equalization, whereas (b) represents the battery pack discharging along with the equalization.

4.7 CHAPTER SUMMARY

In order to keep the battery system functioning well and preserving its health, this chapter discusses the vital requirement for effective cell balancing in battery packs. In order to do this, a unique topology that combines the features of Cuk and buck-boost converters was introduced. By reducing the number of components needed, this integrated approach not only increases efficiency but also makes the design more affordable and compact. The comparison of the three topologies is presented in Table 4,3, where it is evident that Buck-Boost + Cuk outperforms the other two. This topology has several important benefits, one of which is its faster balancing speed. It achieves a cell balancing time of about 0.4 seconds, which is significantly faster than conventional approaches. The chapter also looks at how the circuitry for cell balancing might incorporate a battery charger that is based on a SEPIC converter. The system can efficiently handle the charging and discharging procedures thanks to this connection.

Using MATLAB/Simulink simulations, the combined functionality of the cell balancing and charging circuits was thoroughly assessed. The outcomes show how well the Buck-Boost + Cuk converter cell balancing topology works with the SEPIC converter-based charger, as well as how reliable it is. These simulations verified that the integrated system successfully balances the cells in 0.4 seconds and controls the charging and discharging procedures, demonstrating the design's robustness and practical application.

	Buck-Boost	**Cuk**	**Buck-Boost + Cuk**
Switches employed	2N-2	2N-2	**N**
Inductors employed	N-1	N-1	**N/2**
Capacitors employed	0	N-1	**N/2-1**
Voltage Stress	2 V_{Batt}	2 V_{Batt}	**2 V_{Batt}**
Control logic	Simple	Simple	**Simple**
Balancing speed	Fast	Fast	**Faster**
Balancing efficiency	High	High	**High**
Size and Cost	Large	Large	**Medium**
Modularization	Yes	Yes	**Yes**

Table 4.3: Comparisons of several existing battery equalizers

CHAPTER 5
CONCLUSION AND FUTURE SCOPE

5.1 CONCLUSION

The fundamental problem of cell imbalance in lithium-ion batteries was addressed in this work, which is necessary to preserve the performance and health of the battery. Cell imbalances can result in overcharging or deep draining of individual cells, which can lower capacity, pose safety risks, and shorten battery life. Cell imbalances can be caused by differences in manufacturing, aging, and operating conditions. Techniques for cell balancing are required to lessen these problems. The literature review examined a number of cells balancing techniques, such as switching capacitor, passive, and active approaches.

The primary objective was to develop an efficient and effective cell balancing method. A Zero Current Switching (ZCS) switched capacitor circuit was proposed and integrated with a bi-directional buck-boost charging system. The purpose of this integration was to manage the battery pack's charging and discharging procedures while also increasing balancing efficiency and speed. With a 1.6-second balancing time reduction and improved system performance, the ZCS switching capacitor circuit showed notable benefits.

On top of this base, a cell balancing architecture was presented that combines the advantages of Cuk and buck-boost converters. This method not only makes use of the advantages of both converter types, but it also improves efficiency and lowers the number of components, which results in a more affordable and compact system. Compared to traditional approaches, the integrated system achieved a balancing time of about 0.4 seconds, which is noticeably faster.

Moreover, the cell balancing circuitry incorporated the battery charger based on a SEPIC converter. Operating in buck mode to step down the input voltage during charging and in boost mode to step up the battery voltage during discharging, the SEPIC converter effectively handled both the charging and discharging processes. Its double purpose guaranteed peak efficiency and efficient use of energy.

Detailed MATLAB/Simulink simulations were used to confirm the thorough design and integration of the cell balancing and charging circuits. The outcomes validated the effectiveness and dependability of the suggested system, exhibiting proficient cell balancing in 1.6 seconds for the primary system and 0.4 seconds for the secondary one, signifying efficient management of battery charging and discharging. This work highlights the potential for enhancing the performance and protection of lithium-ion battery packs by demonstrating the durability and practical applicability of the integrated cell balancing and charging system.

5.2 FUTURE SCOPE

This thesis's study has established a strong basis for future developments in lithium-ion battery management systems and cell balancing. Future research can take a number of approaches to expand on these discoveries and improve the effectiveness, efficiency, and practicality of the suggested solutions.

1) **Integration of Thermal Management**: Lithium-ion batteries are currently preferred due to their high-power density, extended life cycle, quick charging time, low self-discharge rate, and high energy density. They are vulnerable to high operating temperatures, though, which can have an adverse effect on the battery's overall life cycle and state of charge (SoC). To lessen these consequences, future research could concentrate on incorporating temperature management techniques into the battery management system (BMS). The suggested charge equalizing strategies might be improved to preserve battery health and lengthen battery life by taking temperature factors into consideration.
2) **Advanced Control Algorithms**: To further enhance the balancing and charging procedures, future study may examine the creation of more complex control algorithms, such as adaptive control or machine learning-based methods. These algorithms have the potential to improve the system's overall performance and efficiency by dynamically optimizing the operational parameters in real-time.

3) **Hardware and Experimental Validation**: Although Simulink simulations have been used to evaluate the suggested active balancing techniques, a thorough experimental testing program is essential to verify these findings in practical settings. These tests would confirm the simulation results and shed light on the real-world difficulties and constraints facing the suggested system. To verify that the balancing approaches are reliable and resilient, real battery packs would be tested in a variety of circumstances.

The suggested cell balancing and charging systems can be further refined to satisfy the changing needs of contemporary energy storage and management applications by addressing these future research objectives. These developments will help create battery management systems that are more effective, dependable, and adaptable, which will eventually encourage a wider use of lithium-ion batteries across a range of industries.

REFERENCES

[1] Xing, Yinjiao, Eden WM Ma, Kwok L. Tsui, and Michael Pecht. "Battery management systems in electric and hybrid vehicles." *Energies* 4, no. 11 (2011): 1840-1857.

[2] Maleki, Hossein, and Jason N. Howard. "Effects of overdischarge on performance and thermal stability of a Li-ion cell." *Journal of power sources* 160, no. 2 (2006): 1395-1402.

[3] Lu, Languang, Xuebing Han, Jianqiu Li, Jianfeng Hua, and Minggao Ouyang. "A review on the key issues for lithium-ion battery management in electric vehicles." *Journal of power sources* 226 (2013): 272-288.

[4] Cao, Jian, Nigel Schofield, and Ali Emadi. "Battery balancing methods: A comprehensive review." In *2008 IEEE Vehicle Power and Propulsion Conference*, pp. 1-6. IEEE, 2008.

[5] Zhi-Guo, Kong, Zhu Chun-Bo, Lu Ren-Gui, and Cheng Shu-Kang. "Comparison and evaluation of charge equalization technique for series connected batteries." In *2006 37th IEEE Power Electronics Specialists Conference*, pp. 1-6. IEEE, 2006.

[6] Zhang, Yongzhi, Rui Xiong, Hongwen He, and Weixiang Shen. "Lithium-ion battery pack state of charge and state of energy estimation algorithms using a hardware-in-the-loop validation." *IEEE Transactions on Power Electronics* 32, no. 6 (2016): 4421-4431.

[7] Moo, Chin S., Yao Ching Hsieh, and I. S. Tsai. "Charge equalization for series-connected batteries." *IEEE Transactions on Aerospace and Electronic Systems* 39, no. 2 (2003): 704-710.

[8] Rui, Ling, Wang Lizhi, Huang Xueli, Dan Qiang, and Zhang Jie. "A review of equalization topologies for lithium-ion battery packs." In *2015 34th Chinese Control Conference (CCC)*, pp. 7922-7927. IEEE, 2015.

[9] Phung, Thanh Hai, Alexandre Collet, and Jean-Christophe Crebier. "An optimized topology for next-to-next balancing of series-connected lithium-ion cells." *IEEE transactions on power electronics* 29, no. 9 (2013): 4603-4613.

[10] Sun, Fengchun, Rui Xiong, and Hongwen He. "A systematic state-of-charge estimation framework for multi-cell battery pack in electric vehicles using bias correction technique." *Applied Energy* 162 (2016): 1399-1409.

[11] Park, Hong-Sun, Chol-Ho Kim, Ki-Bum Park, Gun-Woo Moon, and Joong-Hui Lee. "Design of a charge equalizer based on battery modularization." *IEEE Transactions on Vehicular Technology* 58, no. 7 (2009): 3216-3223.

[12] Pascual, Cesar, and Philip T. Krein. "Switched capacitor system for automatic series battery equalization." In *Proceedings of APEC 97-Applied Power Electronics Conference*, vol. 2, pp. 848-854. IEEE, 1997.

[13] Ye, Yuanmao, and Ka Wai Eric Cheng. "An automatic switched-capacitor cell balancing circuit for series-connected battery strings." *Energies* 9, no. 3 (2016): 138.

[14] Baughman, Andrew C., and Mehdi Ferdowsi. "Double-tiered switched-capacitor battery charge equalization technique." *IEEE Transactions on Industrial Electronics* 55, no. 6 (2008): 2277-2285.

[15] Baughman, Andrew, and Mehdi Ferdowsi. "Analysis of the double-tiered three-battery switched capacitor battery balancing system." In *2006 IEEE Vehicle Power and Propulsion Conference*, pp. 1-6. IEEE, 2006.

[16] Lee, Yuang-Shung, and Ming-Wang Cheng. "Intelligent control battery equalization for series connected lithium-ion battery strings." *IEEE Transactions on Industrial electronics* 52, no. 5 (2005): 1297-1307.

[17] Baronti, Federico, Roberto Roncella, and Roberto Saletti. "Performance comparison of active balancing techniques for lithium-ion batteries." *Journal of Power Sources* 267 (2014): 603-609.

[18] Lee, Wai Chung, David Drury, and Phil Mellor. "Comparison of passive cell balancing and active cell balancing for automotive batteries." In *2011 IEEE Vehicle Power and Propulsion Conference*, pp. 1-7. IEEE, 2011.

[19] Kim, Moon-Young, Chol-Ho Kim, Jun-Ho Kim, and Gun-Woo Moon. "A chain structure of switched capacitor for improved cell balancing speed of lithium-ion batteries." *IEEE Transactions on Industrial Electronics* 61, no. 8 (2013): 3989-3999.

[20] Daowd, Mohamed, Mailier Antoine, Noshin Omar, Peter Van den Bossche, and Joeri Van Mierlo. "Single switched capacitor battery balancing system enhancements." *Energies* 6, no. 4 (2013): 2149-2174.

[21] Yuanmao, Ye, Ka Wai Eric Cheng, and Y. P. B. Yeung. "Zero-current switching switched-capacitor zero-voltage-gap automatic equalization system for series battery string." *IEEE transactions on power electronics* 27, no. 7 (2011): 3234-3242.

[22] Shang, Yunlong, Qi Zhang, Naxin Cui, and Chenghui Zhang. "A cell-to-cell equalizer based on three-resonant-state switched-capacitor converters for series-connected battery strings." *Energies* 10, no. 2 (2017): 206.

[23] Ye, Yuanmao, and Ka Wai Eric Cheng. "Analysis and design of zero-current switching switched-capacitor cell balancing circuit for series-connected battery/supercapacitor." *IEEE Transactions on Vehicular Technology* 67, no. 2 (2017): 948-955.

[24] Sano, Kenichiro, and Hideaki Fujita. "A resonant switched-capacitor converter for voltage balancing of series-connected capacitors." In *2009 International Conference on Power Electronics and Drive Systems (PEDS)*, pp. 683-688. IEEE, 2009.

[25] Tang, Ming, and Thomas Stuart. "Selective buck-boost equalizer for series battery packs." *IEEE Transactions on Aerospace and Electronic Systems* 36, no. 1 (2000): 201-211.

[26] Nishijima, K., H. Sakamoto, and K. Harada. "A PWM controlled simple and high-performance battery balancing system." In *2000 IEEE 31st Annual Power Electronics Specialists Conference. Conference Proceedings (Cat. No. 00CH37018)*, vol. 1, pp. 517-520. IEEE, 2000.

[27] Ye, Yuanmao, and Ka Wai E. Cheng. "Modeling and analysis of series–parallel switched-capacitor voltage equalizer for battery/supercapacitor strings." *IEEE journal of emerging and selected topics in power electronics* 3, no. 4 (2015): 977-983.

[28] Shang, Yunlong, Chenghui Zhang, Naxin Cui, and Josep M. Guerrero. "A cell-to-cell battery equalizer with zero-current switching and zero-voltage gap based on quasi-resonant LC converter and boost converter." *IEEE Transactions on Power Electronics* 30, no. 7 (2014): 3731-3747.

[29] Ye, Yuanmao, Ka Wai E. Cheng, Yat Chi Fong, Xiangdang Xue, and Jiongkang Lin. "Topology, modeling, and design of switched-capacitor-based cell balancing systems and their balancing exploration." *IEEE Transactions on Power Electronics* 32, no. 6 (2016): 4444-4454.

[30] Ohno, Takuya, Takahumi Suzuki, and Hirotaka Koizumi. "Modularized LC resonant switched capacitor cell voltage equalizer." In *IECON 2014-40th Annual Conference of the IEEE Industrial Electronics Society*, pp. 3156-3162. IEEE, 2014.

[31] Shin, Jong-Won, Gab-Su Seo, Chang-Yoon Chun, and Bo-Hyung Cho. "Selective flyback balancing circuit with improved balancing speed for series connected lithium-ion batteries." In *The 2010 International Power Electronics Conference-ECCE ASIA-*, pp. 1180-1184. IEEE, 2010.

[32] Wu, Tsung-Hsi, Chu-Shen Chang, and Chin-Sien Moo. "A charging scenario for parallel buck-boost battery power modules with full power utilization and charge equalization." In *2015 IEEE International Conference on Industrial Technology (ICIT)*, pp. 860-865. IEEE, 2015.

[33] Karuppiah, M., P. Dineshkumar, and K. Karthikumar. "Design a electric vehicle charger based sepic topology with PI controller." In *2020 IEEE International Conference on Advances and Developments in Electrical and Electronics Engineering (ICADEE)*, pp. 1-5. IEEE, 2020.

[34] Ling, Rui, Yan Dong, Hebiao Yan, Meirong Wu, and Yi Chai. "Fuzzy-PI control battery equalization for series connected lithium-ion battery strings." In *Proceedings of The 7th International Power Electronics and Motion Control Conference*, vol. 4, pp. 2631-2635. IEEE, 2012.

[35] Yan, Jingyu, Zhu Cheng, Guoqing Xu, Huihuan Qian, and Yangsheng Xu. "Fuzzy control for battery equalization based on state of charge." In *2010 IEEE 72nd Vehicular Technology Conference-Fall*, pp. 1-7. IEEE, 2010.

[36] Buccolini, Luca, Simone Orcioni, Sauro Longhi, and Massimo Conti. "Cell battery emulator for hardware-in-the-loop bms test." In *2018 IEEE International Conference on Environment and Electrical Engineering and 2018 IEEE Industrial and Commercial Power Systems Europe (EEEIC/I&CPS Europe)*, pp. 1-5. IEEE, 2018.

[37] Lee, Wai Chung, and David Drury. "Development of a hardware-in-the-loop simulation system for testing cell balancing circuits." *IEEE Transactions on Power Electronics* 28, no. 12 (2013): 5949-5959.

[38] Lee, Yuang-Shung, Chun-Yi Duh, Guo-Tian Chen, and Shen-Ching Yang. "Battery equalization using bi-directional Cuk converter in DCVM operation." In *2005 IEEE 36th Power Electronics Specialists Conference*, pp. 765-771. IEEE, 2005.

[39] Chen, Yang, Xiaofang Liu, Yangyi Cui, Jiming Zou, and Shiyan Yang. "A multiwinding transformer cell-to-cell active equalization method for lithium-ion batteries with reduced number of driving circuits." *IEEE Transactions on Power Electronics* 31, no. 7 (2015): 4916-4929.

[40] Farzan Moghaddam, Ali, and Alex Van den Bossche. "An efficient equalizing method for lithium-ion batteries based on coupled inductor balancing." *Electronics* 8, no. 2 (2019): 136.

LIST OF PUBLICATIONS

Paper	Author list. Title. Conference	Status
[1]	Archit Chauhan, Sudarshan K. Valluru, Vanjari Venkata Ramana, **"ZCS Switched-Capacitor Cell Balancing Circuit With Bidirectional Buck-Boost Charging"** IEEE International Conference on Electronics, Computing and Communication Technologies (CONECCT 2024)	Accepted

Gmail Archit chauhan <chauhanarchit208@gmail.com>

[CONECCT 2024] Your paper #1571019090 ('ZCS Switched-Capacitor Cell Balancing Circuit With Bidirectional Buck-Boost Charging')

1 message

Edas Help <help@edas.info> 2 June 2024 at 06:50
To: Archit Chauhan <chauhanarchit208@gmail.com>, Sudarshan Kumar Babu Valluru <sudarshan_valluru@dce.ac.in>, Vanjari Venkata Ramana <venkat.vr90@gmail.com>

Dear Mr. Archit Chauhan:

Congratulations - your paper #1571019090 ('ZCS Switched-Capacitor Cell Balancing Circuit With Bidirectional Buck-Boost Charging') for CONECCT 2024 has been **accepted** and will be presented in IEEE CONECCT 2024.

Please prepare the camera-ready manuscript and upload the same in EDAS by June 11, 2024.

Note that authors must register before uploading the camera-ready manuscript. More details will follow soon.

The reviews are below or can be found at 1571019090.

Review Form 1

Novelty and Originality: What are the positive aspects of the paper?

Author has represented well structured methodology using zero current switching (ZCS) for switched capacitor (SC) cell balancing system's with a bi-directional battery charger circuit. The performance of the proposed system is represented by its balancing speed is independent of both the initial imbalance in cell voltage distribution and the quantity of battery cells.

Originality: What are the Negative aspects of the paper?

1. the work represented in this paper is the investigation and study of ZCS
2. Experimental of the proposed system is preferred than the simulation work

Suggestion: Please suggest authors your view points (for improvement)

1. Experimental results are expected to validate the simulation results
2. Methodology for the tuning of PI controller is missing

Structure/Presentation: Is paper Structured and Organized Properly?

Good (3)

Standard of English: How do you rate the standard of English used in preparing manuscript?

Good (3)

Relevance to Conference: Is topic relevant and within the scope of the conference?

Good (Relevant) (3)

Novelty: Rate the novelty level of this work

Little novelty (3)

Contribution: Rate the contribution to academic debate

Boarder (2)

Appropriateness of abstract as a description of the paper: Rate the appropriateness of abstract as a description of the paper

PAPER NAME

2K22_PES_05_Archit_Chauhan_Thesis.pdf

AUTHOR

Archit Chauhan

WORD COUNT

18536 Words

CHARACTER COUNT

99869 Characters

PAGE COUNT

94 Pages

FILE SIZE

2.0MB

SUBMISSION DATE

Jun 6, 2024 2:38 PM GMT+5:30

REPORT DATE

Jun 6, 2024 2:39 PM GMT+5:30

10% Overall Similarity

The combined total of all matches, including overlapping sources, for each database.

- 7% Internet database
- 6% Publications database
- Crossref database
- Crossref Posted Content database
- 7% Submitted Works database

Excluded from Similarity Report

- Bibliographic material
- Small Matches (Less then 8 words)
- Manually excluded text blocks